Report of Investigations No. 151

THE VAN HORN MOUNTAINS CALDERA, TRANS-PECOS TEXAS:

Geology and Development of a Small (10-km^2) Ash-Flow Caldera

Christopher D. Henry and Jonathan G. Price

1986

BUREAU OF ECONOMIC GEOLOGY • W. L. FISHER, DIRECTOR

Texas Mining and Mineral Resources Research Institute
The University of Texas at Austin • Austin, Texas 78713

Report of Investigations No. 151

THE VAN HORN MOUNTAINS CALDERA, TRANS-PECOS TEXAS:

Geology and Development of a Small (10-km^2) Ash-Flow Caldera

Christopher D. Henry and Jonathan G. Price

Research for this project was supported by the Texas Mining and Mineral Resources Research Institute, through the U.S. Department of the Interior, U.S. Bureau of Mines, under grant numbers G1124148, G1134148, and G1144148.

1986

BUREAU OF ECONOMIC GEOLOGY • W. L. FISHER, DIRECTOR

Texas Mining and Mineral Resources Research Institute
The University of Texas at Austin • Austin, Texas 78713

Cover photograph: View of the western margin of the Van Horn Mountains caldera. High Lonesome Peak is the highest point in the center.

CONTENTS

Figures

Tables

Plate

ABSTRACT

The Van Horn Mountains caldera is a small (~10-km^2) igneous center in the Trans-Pecos volcanic province. The caldera formed 37 to 38 mya during eruption of the first of two ash-flow tuffs related to the caldera. Part of the first tuff ponded within the caldera; the lower marker horizon of the Chambers Tuff in the Sierra Vieja south of the Van Horn Mountains is probably the correlative outflow tuff. Following collapse, the caldera was partly filled by a heterogeneous assemblage of air-fall tuff, tuffaceous sediment, and possible ash-flow tuff. Contemporaneous with this filling, a rhyolite porphyry was emplaced in the middle of the caldera. The porphyry is comparable to the resurgent dome of other calderas but does not uplift the intruded rocks. An intrusive-extrusive complex of basalt, trachyte, and minor rhyolite was emplaced just outside the eastern margin of the caldera; flows from this complex spilled over the rim and into the caldera. Eruption of a second major ash-flow tuff, herein named the High Lonesome Tuff, may have led to additional collapse.

Collapse occurred dominantly along a single, major, nearly circular fracture zone. Embayments in the fracture zone were influenced by precaldera, largely Laramide structures. Large, commonly brecciated blocks of wall rocks slumped into the caldera and were incorporated into caldera fill. Precaldera topography channeled most of the ash-flow tuff to the south, through a low area in the caldera wall.

The 10-km^2 area of the caldera and the no more than 10-km^3 total volume of erupted ash-flow tuff make it one of the smallest ash-flow calderas worldwide and more comparable to collapse features associated with stratovolcanoes. Nevertheless, it shows all the features typical of much larger volcanic centers.

No known ore deposits are associated with the caldera, but the rhyolite porphyry is hydrothermally altered, exhibiting silicification and sericitization typical of many porphyry molybdenum deposits. The apparent lack of deposits may be a function of the small size of the magmatic system, lack of sufficient trace element enrichment by differentiation, or lack of exposure resulting from minimal erosion.

KEYWORDS: ash-flow tuff, caldera, igneous rocks, K-Ar, Trans-Pecos Texas

INTRODUCTION

The Van Horn Mountains caldera is a small (~10-km^2) igneous center in the Trans-Pecos volcanic province within the Van Horn Mountains, a Basin and Range horst (figs. 1, 2; plate). The caldera was the source of two ash-flow tuffs; caldera formation occurred during eruption of the first about 38 mya. Subsequently, the caldera was filled with a heterogeneous assemblage of air-fall tuff, tuffaceous sediment, basaltic to trachytic lava flows, and the second ash-flow tuff; the caldera fill was intruded by a rhyolite dome, and a trachytic to basaltic plug was emplaced just outside the eastern margin of the caldera. Early mapping of the Van Horn Mountains by Twiss (1959a,b) drew our attention to the area as a place for further study of volcanism in Trans-Pecos Texas. Although we have revised some of his work, we owe much to his thorough and accurate study.

This caldera is particularly interesting because of its small size. Its collapse area of about 10 km^2 makes it one of the smallest of epicontinental ring structures, or "ash-flow calderas," and more like typical stratovolcanoes (Smith, 1979; Lipman, 1984; Wood, 1984). Nevertheless, it shows all the features of much larger ash-flow calderas and clearly is one.

Regional Setting

The Van Horn Mountains caldera lies in the northwestern part of the Trans-Pecos volcanic province (fig. 1). The province is dominantly late Eocene to early Oligocene (38 to 32 m.y.) in age, but activity extended from 48 to 17 mya (Henry and McDowell, 1986). In a regional context, the Trans-Pecos province is part of a major volcanic province that extends westward from Texas across Chihuahua and to the Sierra Madre Occidental of western Mexico. It is generally accepted that the igneous rocks of this province were generated by processes related to subduction (Coney and Reynolds, 1977; Damon and others, 1981). A paleo-

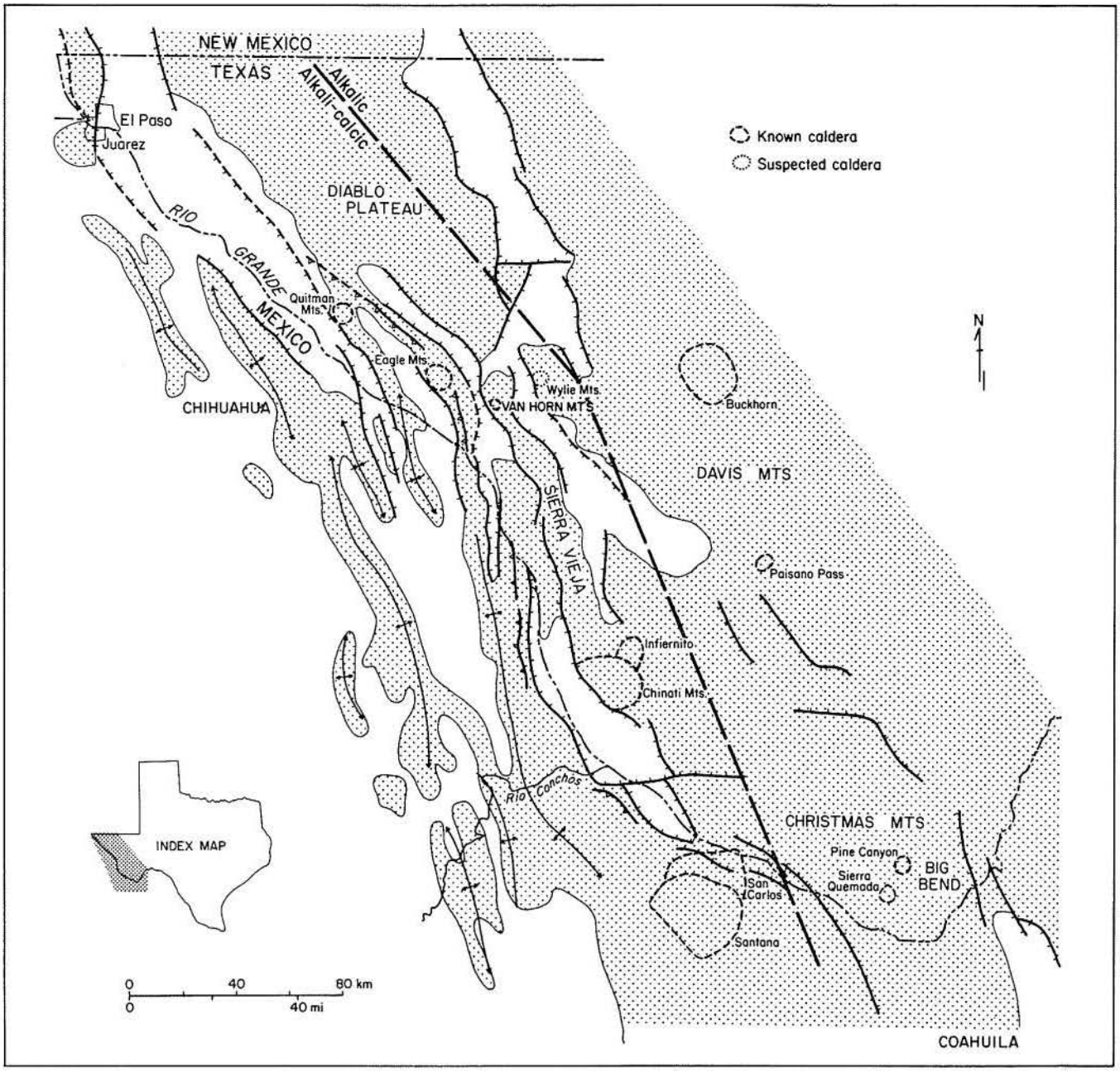

FIGURE 1. Location of the Van Horn Mountains caldera in the volcanic field of Trans-Pecos Texas.

trench for this subduction lay off the west coast of Mexico. Igneous activity swept eastward from near the present Pacific coast about 100 mya to Trans-Pecos Texas about 40 to 30 mya and then either swept rapidly back to the coast or flared up nearly simultaneously across almost all of western Mexico (Coney and Reynolds, 1977; Keith, 1978; Damon and others, 1981; Henry and McDowell, 1982). Subduction-related activity terminated near the west coast of Mexico about 20 mya.

The Trans-Pecos part of this larger province is characterized by several major volcanic centers, commonly calderas or caldera complexes, and by numerous small intrusive centers with little or no associated volcanic rocks. The calderas were the sources of silicic ash-flow tuffs, and caldera areas are characterized by thick ash-flow tuffs, by thick sequences of lava flows, especially where they fill the calderas, and by numerous intrusions related to the calderas. Tuffaceous sediments, probably derived by erosion

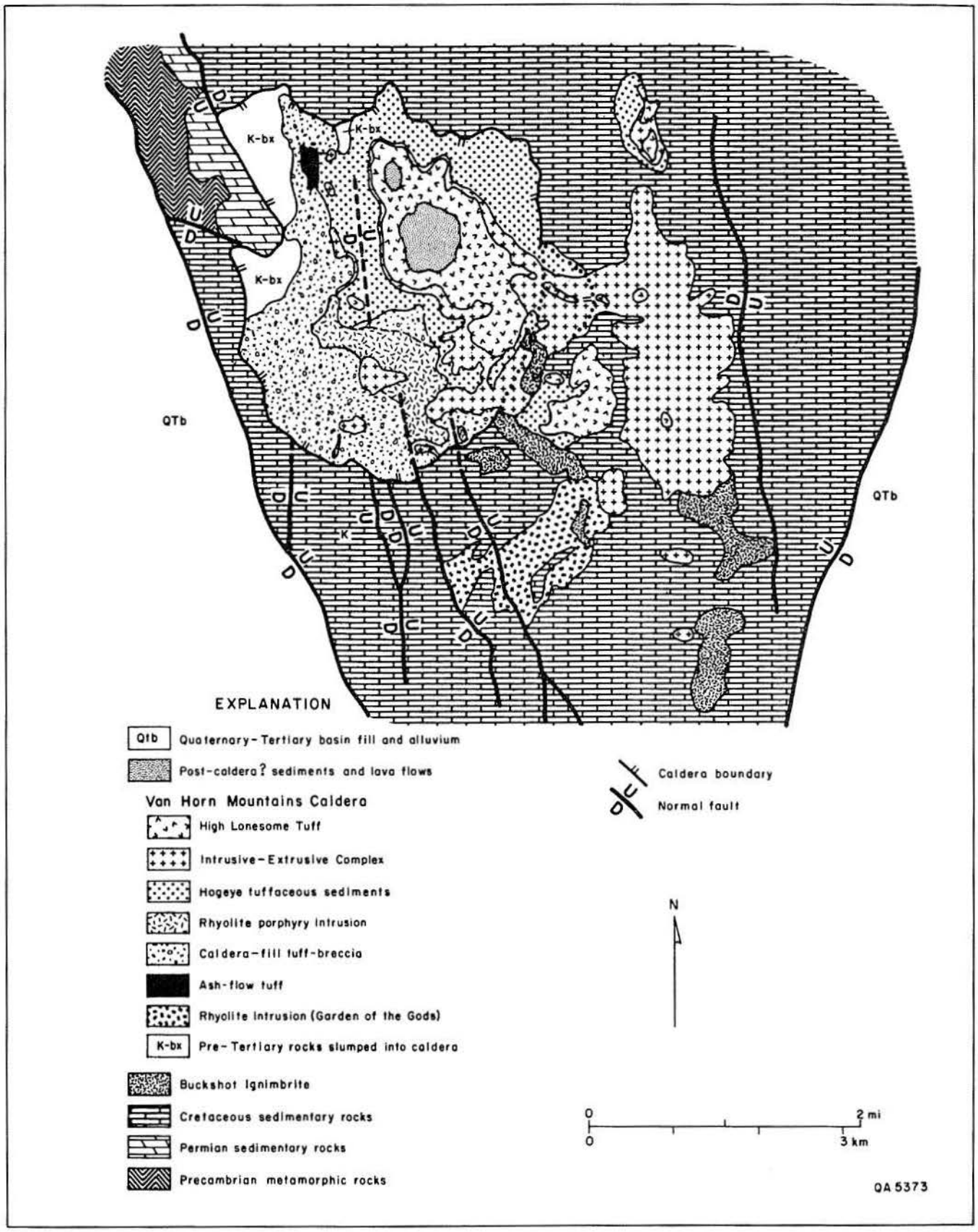

FIGURE 2. Generalized geologic map of the Van Horn Mountains caldera.

from air-fall and ash-flow tuffs from the calderas, were redeposited as alluvial fans and other deposits in broad aprons between calderas (Walton, 1975, 1979). A few mostly thin, throughgoing ash-flow tuffs and lava flows are interbedded within the tuffaceous sedimentary sequences. Intrusive clusters unrelated to calderas occur in several areas, most notably in the Christmas Mountains – Big Bend area but also in the southern Davis Mountains, north of the Quitman Mountains, in the Diablo Plateau, and in the Hueco Tanks area east of El Paso. Alkalic, silicic to intermediate stocks and laccoliths are common in all these areas; more mafic intrusions are common only in the Christmas Mountains – Big Bend area and in the Diablo Plateau. The intrusions are commonly small (less than a few kilometers in diameter) and were emplaced at very shallow depths. Extrusive equivalents either are not present or are minor. Probably these intrusions lacked significant associated extrusive activity.

The Van Horn Mountains caldera occurs in the northern part of the Van Horn Mountains, which are separated by major normal faults from basins filled with up to a kilometer of upper Tertiary sediments. The area is a major structural high; Precambrian rocks crop out in the Van Horn Mountains and in several nearby Basin and Range horsts. In most other areas of Trans-Pecos, Precambrian rocks occur only deep in the subsurface.

Purpose

The purpose of the study that led to this report is twofold: (1) to understand the development of the igneous rocks of Trans-Pecos Texas and their regional tectonic setting and (2) to determine the geologic processes and settings in Trans-Pecos Texas that give rise to ore deposits. This report focuses on the Van Horn Mountains, a small volcanic center.

The Van Horn Mountains caldera was previously recognized as a volcanic center by Twiss (1959a) but not specifically identified as a caldera. As such, it is a small but significant part of the volcanic development of Trans-Pecos Texas and in turn fits into the larger picture of subduction-related magmatism of western North America. Understanding the development of the caldera—including nature, timing, and geochemistry of the igneous rocks and structural development—helps in understanding the development of the entire volcanic province.

In addition, study of the Van Horn Mountains is part of an evaluation of the mineral potential of Trans-Pecos Texas. Much of the mineralization of the region is related to igneous rocks and, more specifically, to calderas. For example, the large Chinati Mountains caldera has several major deposits and numerous prospects, apparently related to caldera structures and magmatism (McAnulty, 1976; Cepeda and Henry, 1983; Price and others, 1983). The Van Horn Mountains caldera has undergone hydrothermal alteration but appears to have no genetically related ore deposits. Some nearby silver deposits are unrelated to the igneous activity (Price, 1982). Comparison of the Van Horn Mountains caldera with mineralized calderas should help to identify what particular characteristics of calderas are important in localizing ore deposits, including such characteristics as size, intensity or duration of igneous activity, chemical composition of associated rocks, structure, or host rocks.

STRATIGRAPHY

Because this report is concerned primarily with caldera development, the pre-Cenozoic rocks (fig. 3) are discussed only briefly. However, rocks ranging in age from Proterozoic to Recent are exposed in the Van Horn Mountains (Twiss, 1959b). Major unconformities occur between the Precambrian and Permian, between the Permian and Cretaceous, and between the Cretaceous and Eocene or Oligocene. Although Cretaceous sandstones and limestones formed most of the walls of the early Oligocene Van Horn Mountains caldera, Permian and Proterozoic rocks may have been exposed at the time of eruption because they were incorporated in caldera fill. Formation of the Van Horn Mountains caldera was one of the earliest events in the Tertiary volcanic activity of Trans-Pecos Texas, and almost all igneous rocks near the caldera were derived from it.

Precambrian Rocks

Meta-quartzite, meta-arkose, muscovite schist, biotite schist, amphibolite, and pegmatite of the Carrizo Mountain Group are the oldest rocks in the Van Horn Mountains (Flawn, 1951; King and Flawn, 1953) and probably the oldest rocks in Trans-Pecos Texas. Denison (1980) estimated a depositional age of 1,200 to 1,300 m.y. of the Carrizo Mountain Group on the basis of Rb/Sr isochrons on metarhyolites. Condie (1982) suggested that the Carrizo Mountain Group represents a bimodal (basalt-rhyolite) volcanic assemblage resulting from Proterozoic subduction and continental accretion. Mattison and Rudnick (1982) showed that many of the silicic rocks were originally rhyolitic ash-flow tuffs.

Metamorphism, reaching almandine-amphibolite facies in the Van Horn Mountains but decreasing in grade to the north, probably occurred approximately 1,000 mya (Denison, 1980). A major thermal event

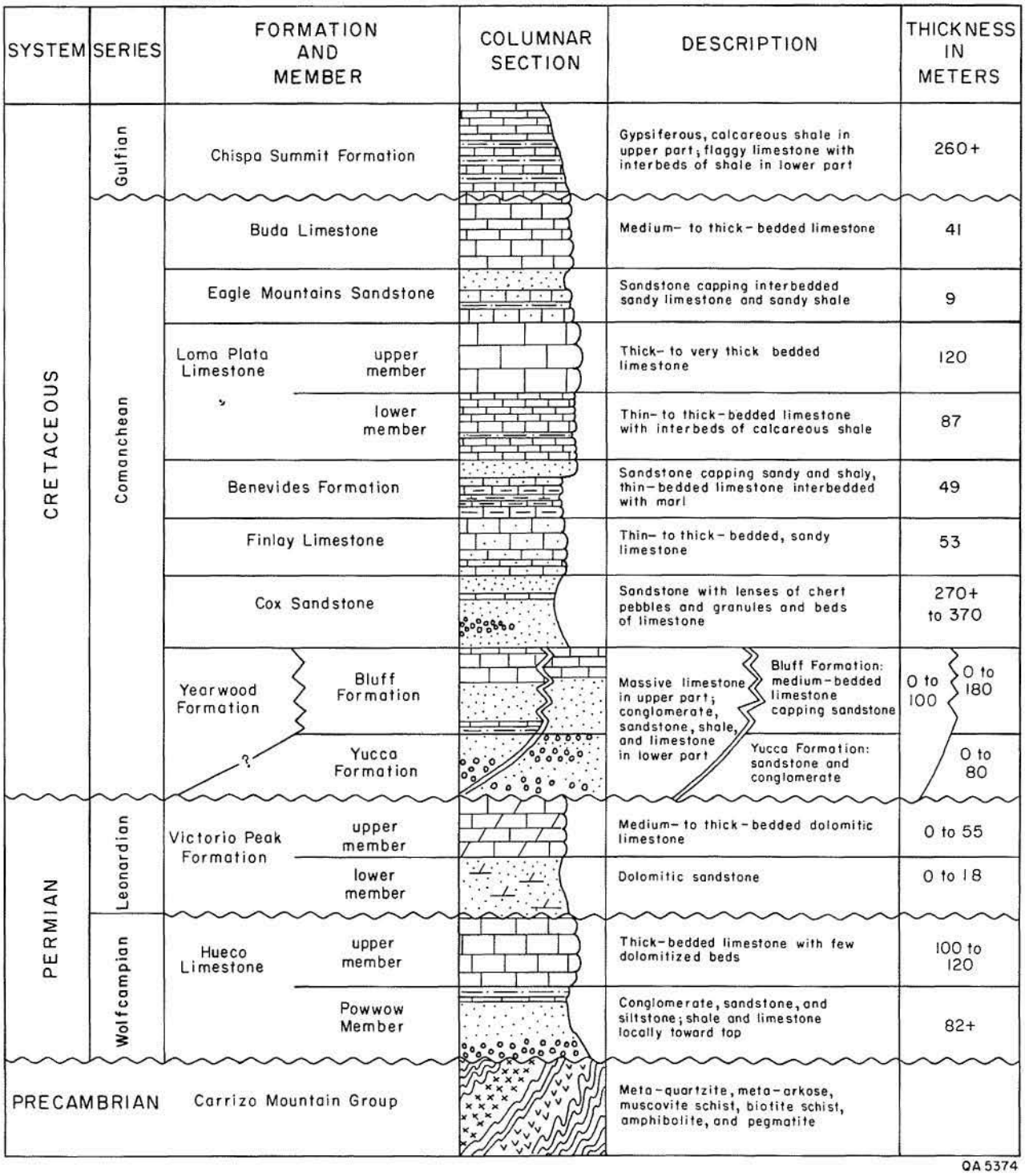

FIGURE 3. Pre-Cenozoic stratigraphic column, Van Horn Mountains, Texas (after Twiss, 1959a).

affected much of the Trans-Pecos region at this time. This Grenville age closely corresponds to ages determined for the granitic and rhyolitic rocks exposed to the northwest at Pump Station Hills and in the Hueco and Franklin Mountains (Denison and Hetherington, 1969).

Permian Rocks

Permian rocks rest unconformably on Precambrian metamorphic rocks in the Van Horn Mountains (Twiss, 1959a, b). Late Pennsylvanian – Early Permian erosion apparently removed older Paleozoic sedimentary

rocks, such as those that crop out in the Sierra Diablo to the north (King, 1965). The oldest and most widespread Paleozoic rock in the Van Horn Mountains is the Hueco Limestone, which is divided into two lithologically distinct units. The lower Powwow Conglomerate Member is composed chiefly of fluvial conglomerates, sandstones, and siltstones, along with minor amounts of limestone and shale near its top. Thickness of the member ranges from zero to at least 82 m (Price, 1982). The upper member of the Hueco Limestone is composed of 100 to 120 m of marine limestone and a few dolomitic limestone lenses (Twiss, 1959a, b). Whereas the unfossiliferous lower part of the Powwow Member may be Pennsylvanian (King, 1934), marine fossils indicate a Wolfcampian (Early Permian) age for the upper part of the Powwow Member and for the overlying Hueco limestones (King, 1934, 1965; Hay-Roe, 1957).

The overlying Victorio Peak Formation crops out over a limited area in the northeastern Van Horn Mountains (Twiss, 1959b), where it attains a thickness of at least 73 m (Twiss, 1959a). It is composed of a basal dolomitic sandstone member and an upper limestone member. On the basis of fossil evidence, Twiss (1959a) noted that a period of erosion existed after deposition of the Hueco Limestone and before deposition of the Victorio Peak Formation in this area. Near the Van Horn Mountains caldera, the Victorio Peak Formation is absent; Cretaceous rocks overlie the Hueco Limestone.

Cretaceous Rocks

The Cretaceous section in the Van Horn Mountains is dominated by sequences of limestones and sandstones (Twiss, 1959a, b) that record transgressive-regressive events (Scott and Kidson, 1977). The section is approximately 1,100 m thick. Twiss (1959a) noted that the Lower Cretaceous strata are transitional between thicker sequences in the Chihuahua Trough to the southwest, where DeFord and Haenggi (1970) noted more than 3,800 m of Jurassic to Cretaceous sedimentary rocks, and the thinner sequence on the Diablo Platform to the northeast. The Chihuahua Trough, of probable Jurassic age, is a deep basin floored by evaporites, which are not exposed in the Van Horn Mountains. Sandstones deposited in coastal plain (Scott and Kidson, 1977) or beach (Twiss, 1959a) environments include those in the Yucca Formation, the lower parts of the Bluff and Yearwood Formations, the Cox Sandstone, and the upper parts of the Benevides Formation and Eagle Mountains Sandstone (fig. 3). Thick marine limestones deposited in mostly shallow water are present in the upper parts of the Bluff and Yearwood Formations, in the Finlay Limestone, the Benevides Formation, the Loma Plata Limestone, and the Buda Limestone (fig. 3).

Tertiary Rocks

Most of the volcanic rocks of the area were derived from the Van Horn Mountains caldera. The Colmena Formation and Buckshot Ignimbrite are precaldera rocks unrelated to the caldera. Some late tuffaceous sediments and trachyte lava flows are discussed in sections dealing with the caldera, although their relationship to it is uncertain.

Colmena Formation

Conglomerate and tuff or tuffaceous sediment of probable Eocene age were mapped by Twiss (1959b) as part of the Colmena Formation and are the oldest Tertiary rocks exposed in the area (fig. 4). Twiss included in the Colmena Formation two units we have mapped separately: an ash-flow tuff we have identified as the Buckshot Ignimbrite and several small, isolated outcrops of basalt. We think the basalts are actually part of an intrusive-extrusive complex of trachyte and basalt emplaced during caldera development. The conglomerates occupy a north-trending valley cut into Cretaceous limestones and sandstones near the southeastern edge of the map area (plate). Twiss measured 5 m of coarse boulder conglomerates and a 15-m covered interval that he thought might be tuff. Clasts in the conglomerate are up to 1 m in diameter and are composed exclusively of Cretaceous rocks. Thus the conglomerate was deposited before significant volcanic activity began in the area, on an erosional surface of at least moderate relief developed on Cretaceous rocks.

Buckshot Ignimbrite

The Oligocene Buckshot Ignimbrite, which overlies and occupies the same valley as the conglomerate of the Colmena Formation (fig. 5), is the oldest volcanic rock in this area. It continues to the southeastern edge of the caldera where it directly overlies the Cretaceous Finlay Limestone. Twiss measured 38 m of Buckshot ash-flow tuff, including 1.5 m of basal vitrophyre, in valley fill at the eastern edge of the map area (plate). This is anomalously thick compared to the regional thickness of the Buckshot, which is at most 19 m thick.

The Buckshot is a peralkaline, rhyolitic ash-flow tuff. It contains a few percent alkali feldspar phenocrysts (2 mm) and 1 percent or less green clinopyroxene. Rock fragments and pumice are less than 1 cm and compose at most 1 or 2 percent of the rock. The valley fill in the southeast has a densely welded base grading upward to a moderately welded top and appears to be both a single cooling unit and a single ash flow. Cavities up to 5 mm across are developed in spherulites; these cavities are the source of the name "Buckshot." Several blister cones (fig. 6), remnants of fumaroles developed on the

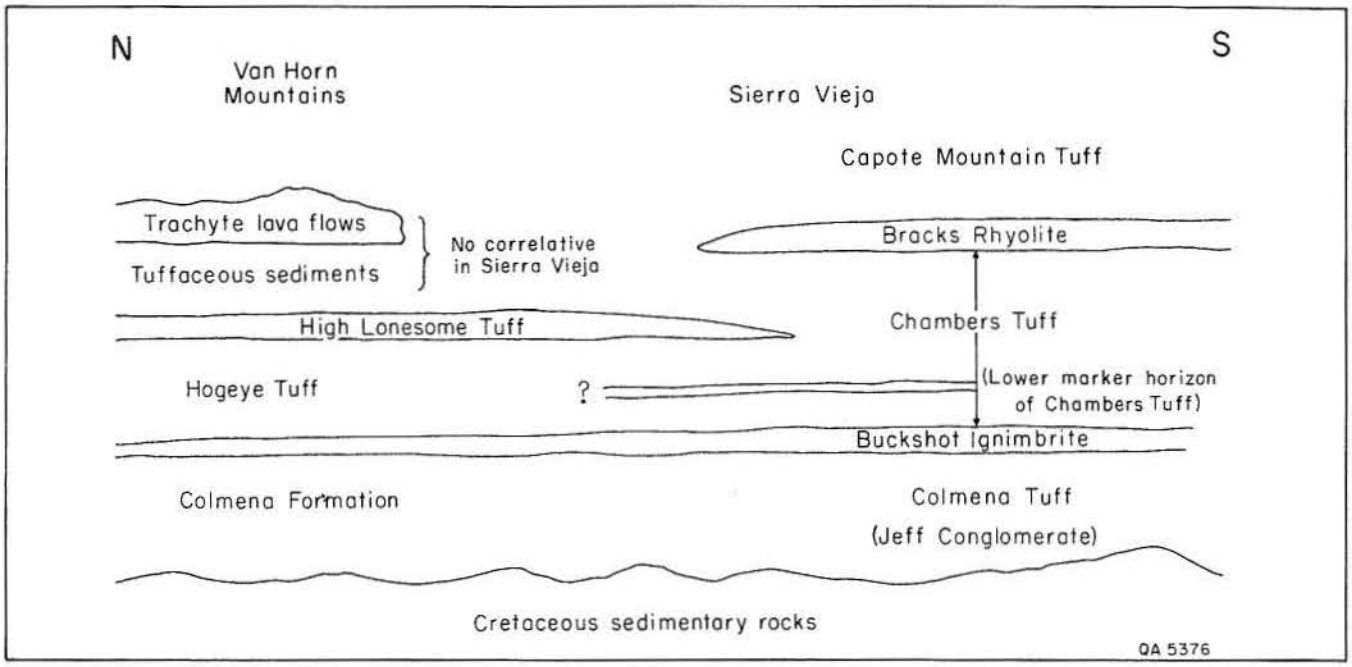

FIGURE 4. Correlation of regional volcanic units, Van Horn Mountains and northern Sierra Vieja. The lower marker horizon of the Chambers Tuff is probably outflow tuff correlative with the caldera-forming ash-flow tuff in the Van Horn Mountains caldera. Not to scale.

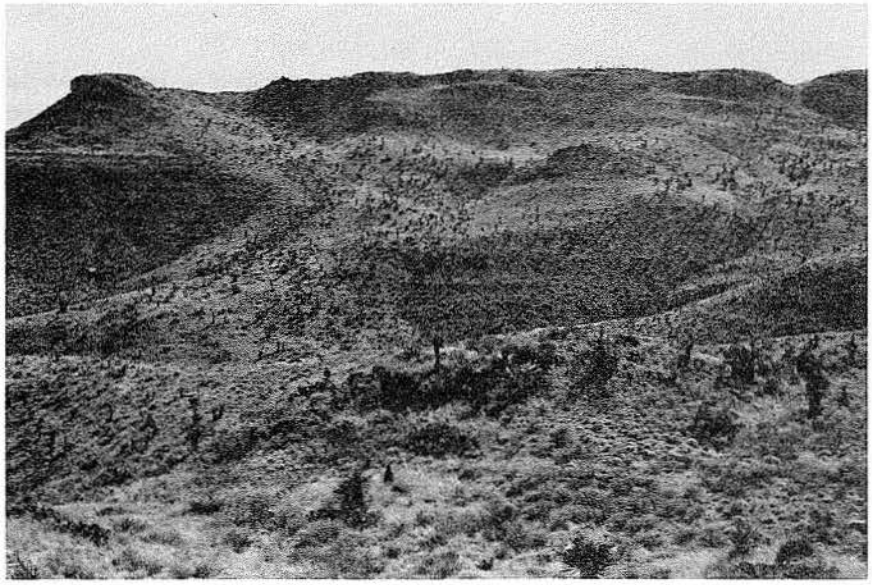

FIGURE 5. Buckshot Ignimbrite overlying conglomerate in Colmena Formation. Both fill a valley that was eroded into flat-lying Cretaceous rocks.

upper surface of the ash-flow tuff during cooling and devitrification, occur in the Buckshot near the caldera wall (Anderson, 1975). The blister cones, which are characteristic of the Buckshot elsewhere, are uplifted and intensely silicified upper parts of the ash-flow tuff. Extensional fractures radiating out from the cones are filled with jasperoidal silica.

The Buckshot Ignimbrite was erupted about 37 to 38 mya from the Infiernito caldera (Duex and Henry, 1981; Henry and Price, 1984; Henry and McDowell,

FIGURE 6. Blister cone on upper surface of the Buckshot Ignimbrite. Radial tension cracks indicate that the Buckshot was solidified by the onset of fumarolic activity.

1986) approximately 90 km to the south in the Chinati Mountains area. The Buckshot was previously not known to crop out in the Van Horn Mountains; these outcrops now constitute its northernmost known occurrence. The Buckshot is unrelated to the Van Horn Mountains caldera for two reasons: (1) the Buckshot is clearly older as it is truncated by the caldera wall. One outcrop of Buckshot appears to have slumped into the caldera and is surrounded by tuff-breccia related to the caldera; (2) the ash-flow tuff that produced the Van Horn Mountains caldera contains abundant biotite, so it cannot be peralkaline, as is the Buckshot.

Rocks of the Van Horn Mountains Caldera

Garden of the Gods Intrusion

A distinctive, gray, flow-banded, sparsely porphyritic rhyolitic intrusion crops out about 1 km from the caldera wall southeast of Carpenter Lodge in the area known as Garden of the Gods (fig. 7). The rhyolite intrudes Cretaceous rocks and volcanic rocks at least as young as the Buckshot Ignimbrite; it was probably emplaced before caldera collapse but is likely part of caldera-related magmatism. Cox Sandstone and Buckshot Ignimbrite both occur as roof pendants in the center of the intrusion. The intrusion is in part concordant and in part discordant. Along the southeastern margin, Loma Plata Limestone is flat lying at the contact. However, along the northwestern margin, Cox Sandstone is recrystallized to a quartzite, dips away from the intrusion, and is structurally uplifted at least 200 m.

Flow-banding and aligned vesicles in the intrusion give the rock a ropy appearance. The banding roughly parallels contacts with country rock and roof pendants. In the center of the intrusion the banding varies from horizontal to undulatory, forming vague anticlines and synclines. The rock contains less than 1 percent total phenocrysts, which consist of 1-mm rounded quartz and alkali feldspar grains. The groundmass is composed of interlocking quartz and alkali feldspar with minor opaque minerals (fig. 8).

The vesicular, flow-banded character and the doming of the host rocks indicate shallow emplacement. Twiss (1959b) mapped this intrusion as part of the rhyolite porphyry intrusion that occurs within the caldera. Although the two intrusions may ultimately have come from the same magma chamber, they are texturally distinct, occur in different settings, and were emplaced at different times.

The major outcrop of the Garden of the Gods rhyolite is outside the caldera and not in contact with rocks that would allow correlation with caldera stratigraphy or evolution. However, trachyte, probably

FIGURE 7. Intrusive contact of Garden of the Gods rhyolite (left) with the Buckshot Ignimbrite (right). Flow banding in the rhyolite dips to the northeast parallel to the contact, and the Buckshot is domed away from the contact.

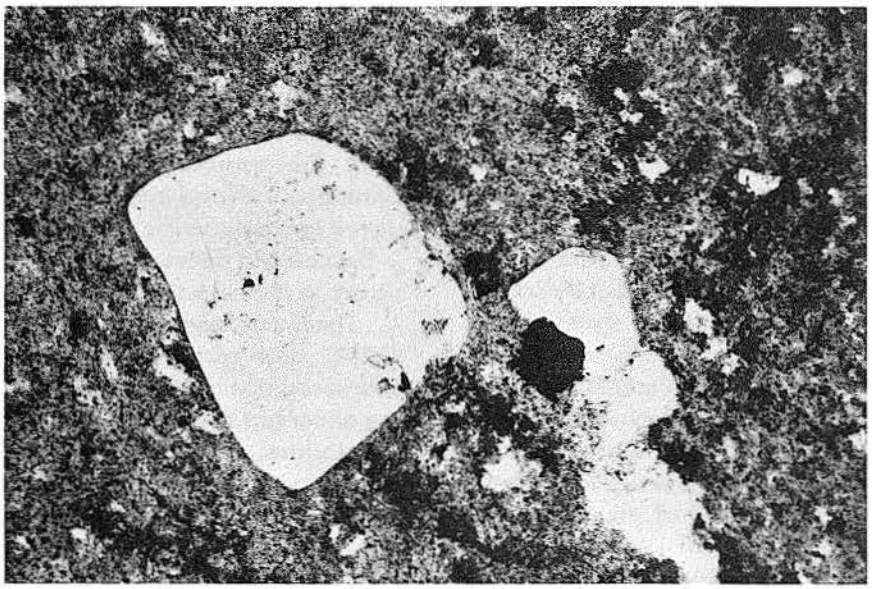

FIGURE 8. Photomicrograph of quartz phenocrysts in a groundmass of quartz, alkali feldspar, and opaque minerals, Garden of the Gods rhyolite. Long dimension is 3.6 mm.

related to an intrusive-extrusive complex emplaced late during caldera evolution, appears to intrude the rhyolite along its northeastern edge. Two small outcrops of rhyolite at the caldera margin about 1 km southwest of Carpenter Lodge appear to form part of the caldera wall and to underlie a large block of Buckshot Ignimbrite believed to be slumped into the caldera. Thus the intrusion is probably precaldera. Some

petrographically similar, flow-banded rhyolite within the caldera is probably part of the younger intrusive-extrusive complex.

Caldera-Forming Ash-Flow Tuff

A rhyolitic ash-flow tuff is the oldest exposed volcanic rock of the caldera; it is also the tuff whose eruption led to caldera collapse. It crops out in a small area (<0.5 km^2) in the northwestern part of the caldera, particularly along the south bank of an arroyo just southwest of the windmill at elevation 4,456 (see plate). The tuff underlies tuffaceous sediments of the Hogeye Tuff and basaltic lava flows that erupted from an intrusive-extrusive complex near the eastern margin of the caldera. It also underlies the tuff-breccia that fills the caldera, but the ash-flow tuff and the tuff-breccia may be related and, at the least, are sufficiently similar in the field that a precise contact is difficult to identify. The base of the ash-flow tuff is not exposed, but it may overlie the Buckshot Ignimbrite within the caldera.

The tuff contains up to 10 percent total phenocrysts, mostly of quartz and lesser alkali feldspar, which range up to 2 mm in diameter. Small (≤ 1 mm) biotite flakes were found in every sample examined; commonly the biotite is oxidized to iron oxides.

Small angular rock fragments, up to about 1 cm in diameter, compose about 5 percent of most samples. Fragments include probable Cretaceous sandstones and limestones (but probably Permian limestones also) and Precambrian metamorphic rock fragments including schist and individual grains of muscovite, microcline, and highly strained quartz.

Glass shards and pumice are unflattened, and in general the ash-flow tuff is nonwelded but indurated (fig. 9a, b). No suggestion of eutaxitic structure was seen in either outcrop or thin section. Shards in one sample are still glassy, but in several others they have been replaced by calcite, probably because limestone is abundant both as fragments and in nearby outcrops. A more welded, lower part of the tuff may underlie the observed exposures and outcrops of other, younger rocks in the caldera.

The total thickness of the tuff is unknown because the base is not exposed. The exposed thickness is no greater than about 30 m but is difficult to estimate because the lack of eutaxitic texture makes the attitude of the tuff impossible to determine. We assume it is nearly flat lying because overlying rocks are. Based on the size of the caldera, the estimated volume of correlative outflow tuff, and comparison with other caldera-filling ash-flow tuffs in Texas, the tuff could be as much as several hundred meters thick and mostly densely welded. The total volume of caldera-fill tuff could then be as much as several cubic kilometers, given the 10-km^2 caldera area. Because observed tuff is nonwelded, equivalent magma volume would be less. However, any correction would be well within the large uncertainty of the original estimate for this and other tuffs.

We suspect that the lower marker horizon of the Chambers Tuff, exposed in the Sierra Vieja to the south, is the equivalent outflow facies of the ash-flow tuff. Evidence for this correlation is presented below. Other possible correlations are unlikely. Several quartz- and feldspar-bearing ash-flow tuffs crop out in the Indio Mountains just 10 km to the west, but these overlie the High Lonesome Tuff (formerly called Pantera Trachyte). The ash-flow tuff in the Van Horn Mountains caldera clearly underlies the High Lonesome Tuff and should overlie the Buckshot Ignimbrite in any outcrops outside the caldera.

Lower Marker Horizon of the Chambers Tuff

The lower marker horizon is an informally designated unit in the Chambers Tuff (DeFord, 1958) that crops out in the Sierra Vieja south of the Van Horn Mountains. Although it does not occur in the Van Horn Mountains, the lower marker horizon is described because it is probably the outflow facies of the ash-flow tuff erupted from and filling the Van Horn Mountains caldera. Walton (1972) considered the lower marker horizon an ash-flow tuff because it is distinctly different from the enclosing tuffaceous sediments of the Chambers Tuff and because it is laterally extensive. We agree and believe it is correlative with the ash-flow tuff in the caldera because it is mineralogically similar and occurs in the appropriate stratigraphic position.

The lower marker horizon, as described by Walton (1972) and corroborated by our investigation, is composed dominantly of angular glass shards containing minor (up to 2 percent total) phenocrysts of quartz, plagioclase, and sanidine. Shards and phenocrysts range up to 0.5 mm in diameter. A photomicrograph (Walton, 1972, p. 77) shows incipient welding of shards around a sanidine phenocryst. The rock is diagenetically altered to clinoptilolite, montmorillonite, and calcite.

The lower marker horizon extends 40 km, from the northern Sierra Vieja, which is about 15 km south of the Van Horn Mountains caldera, to the southern Sierra Vieja. It is laterally continuous, absent only where channeled out, and uniformly 2 to 3 m thick. The lower marker horizon occurs in the Chambers Tuff about one-third of the way upward between the Buckshot Ignimbrite and the Bracks Rhyolite (the upper and lower boundaries of the Chambers Tuff) and about halfway between the Buckshot and the High Lonesome Tuff (fig. 4). We know of no other areas of outcrop, but most

FIGURE 9a. Outcrop of caldera-forming ash-flow tuff showing abundant small rock fragments in a gray, devitrified but nonwelded matrix.

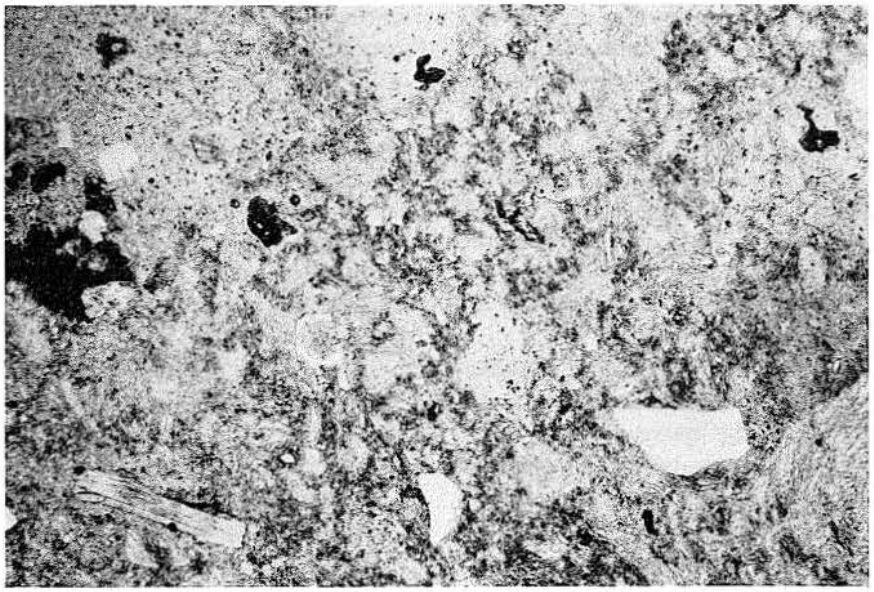

FIGURE 9b. Photomicrograph of caldera-forming ash-flow tuff showing undeformed shards, quartz phenocryst, and a fragment of Precambrian muscovite.

volcanic rocks have been completely removed by erosion elsewhere around the caldera.

We agree with Walton's assessment that the lower marker horizon is an ash-flow tuff. It is probably the ash-flow tuff erupted from the Van Horn Mountains caldera because it is petrographically similar to the tuff within the caldera and it occurs in the proper stratigraphic position. Also, the sedimentary record shows that a volcanic source became active to the north of the Sierra Vieja at the time of deposition of the lower marker horizon (Walton, 1977).

The total volume of the lower marker horizon and therefore outflow equivalent of the caldera-fill tuff is difficult to estimate because even its present distribution is so poorly known. A minimum of about 2 km^3 can be estimated from its occurrence in the Sierra Vieja, which may have been its total original distribution. If the tuff had once been more symmetrically distributed around the caldera, the total volume could have been as much as 30 km^3. Considerations of the size of the source caldera, discussed on page 38, suggest that something close to the lower value is more likely.

Rhyolite Porphyry Intrusion

Most of the south-central part of the caldera is underlain by a white, coarsely porphyritic, rhyolite intrusion. The rhyolite is in part covered by and in part intruded into its own tuffaceous ejecta or debris shed off the rising shallow dome. Petrographically similar dikes occur in two places near the southwest caldera wall, and a lobe extending west from the main outcrop may be a related flow (fig. 10a). Phenocrysts consist of large (5 mm), rounded, embayed bipyramidal quartz (20 percent) and subequal amounts (5 percent total) of sanidine and plagioclase as large as 2 mm in diameter. In all samples the feldspars have been silicified and altered to sericite and a kaolinite-group mineral (fig. 10b). The groundmass consists of a fine mosaic of quartz (in part introduced) and cloudy alkali feldspar. Chemical analyses (table 1, p. 26) also demonstrate silicification. Mafic phenocrysts have been altered to sericite and opaques, but fragments of the porphyry in the tuff-breccia contain a few percent biotite.

The rhyolite porphyry was emplaced at a shallow depth and was partly exposed during emplacement. The rhyolite is overlain in many places by the tuff-breccia (fig. 11). In places along the contact of rhyolite and breccia, lobate dikes of rhyolite prophyry intrude the tuff-breccia (fig. 12), demonstrating that intrusion and formation of the breccia were contemporaneous. Flow banding is rare in most of the intrusion but is present in these dikes, where it parallels contacts. Two other rhyolite porphyry dikes intrude the breccia near the southwestern margin of the caldera (see plate).

A lobe of rhyolite porphyry extending west of the main body of the intrusion may be a flow (fig. 10a). The base is not exposed, but the overall geometry suggests a wide, short flow. Alternatively, it could simply be a lobate dike from the main intrusion.

Tuff-Breccia

A heterogeneous but related assemblage of breccia, conglomerate, and tuff crops out in the southern and western parts of the caldera and probably underlies much of the area under High Lonesome Peak. For want of a better term, we have informally designated this material "tuff-breccia." It is probably in part ash-flow and air-fall tuff. It incompletely fills the caldera, demonstrating that the caldera predates the tuff-breccia. Twiss (1959a) included this material within the Hogeye Tuff and Rhyolite Stock of his study. Our work shows that the tuff-breccia is in part derived from the Rhyolite Stock (our rhyolite porphyry intrusion).

Near the rhyolite porphyry the tuff-breccia consists of angular fragments of rhyolite porphyry, pumice, and minor Cretaceous rocks in a white, tuffaceous matrix that also contains abundant quartz and feldspar fragments (fig. 13). Immediately adjacent to the contact with the porphyry, the tuff-breccia is unbedded and unsorted and grades into brecciated porphyry and then into actual intrusion (fig. 11). The tuff-breccia there appears to be a gravity deposit derived with little transport from the porphyry. At places no more than a few hundred meters from the contact, the tuff-breccia clearly has been reworked by water. The deposits are bedded, are sorted to some degree, and show channels cut into underlying deposits (fig. 14a, b).

Away from contacts with the rhyolite porphyry, the tuff-breccia is nonbedded, coarsely clastic, and unsorted. A variety of rock fragments as large as 30 cm in diameter are in a commonly devitrified matrix containing abundant pumice. Shards are not apparent but may have been destroyed by devitrification. Devitrification and the presence of bleached rims around many clasts suggest that the deposit must have been relatively hot at the time of emplacement.

Near the caldera wall, the tuff-breccia contains extremely large (up to 50 m across) blocks derived from the caldera wall (fig. 15), but it is otherwise similar to tuff-breccia elsewhere. The largest blocks are Cretaceous rocks, including Cox Sandstone and an unidentified limestone (probably Finlay), but smaller fragments of Precambrian rocks and probable Permian Hueco Limestone are also present. The largest blocks must have slumped into the caldera from the oversteepened caldera wall, probably only shortly after caldera subsidence. They are commonly intensely

FIGURE 10a. Possible flow of rhyolite porphyry extending as a flat lobe west of the main mass of the intrusion. The western wall of the caldera is in the background.

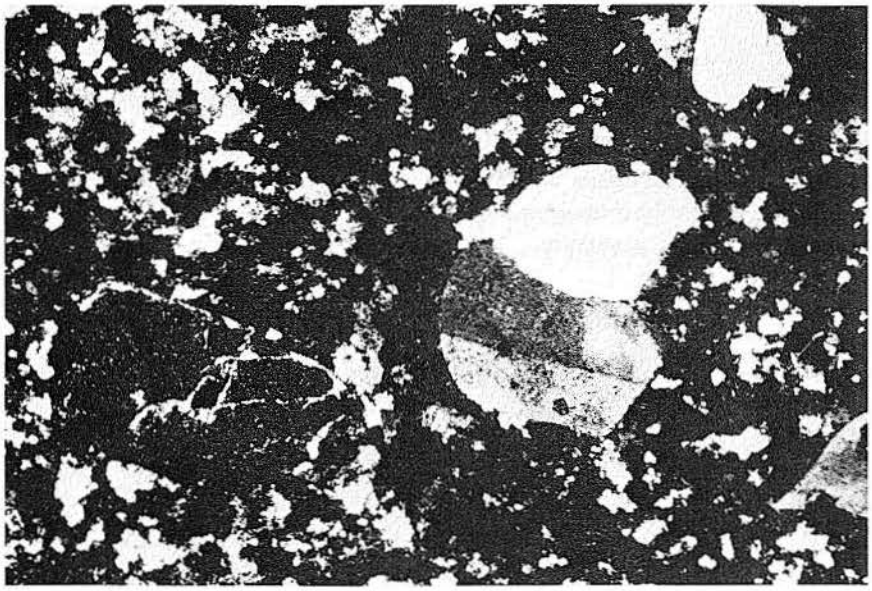

FIGURE 10b. Photomicrograph of rhyolite porphyry with quartz and altered alkali feldspar phenocrysts in a silicified groundmass of quartz and feldspar (crossed nicols). Long dimension is 3.6 mm.

brecciated and recemented. For example, the more than 50-m-long block of Cox Sandstone along the western margin of the caldera has been totally shattered (fig. 16). The fragments within this block range up to 1 m in diameter and are no longer in their original position relative to other fragments. Although brecciation may be due in part to fracturing during Laramide faulting, most of it probably occurred during,

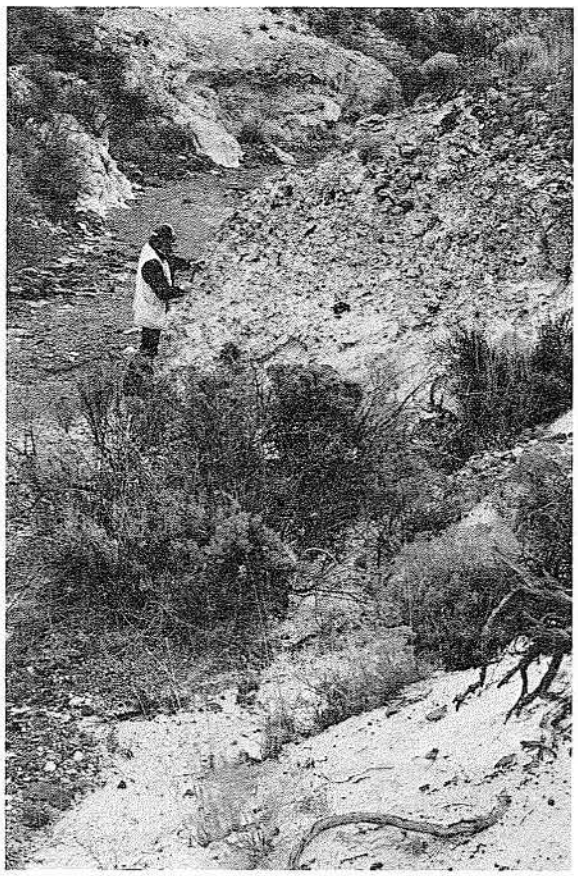

FIGURE 11. Outcrop of rhyolite porphyry (background and lower part of middle ground) overlain by tuff-breccia (upper part of middle ground and foreground) composed of coarse blocks of rhyolite porphyry.

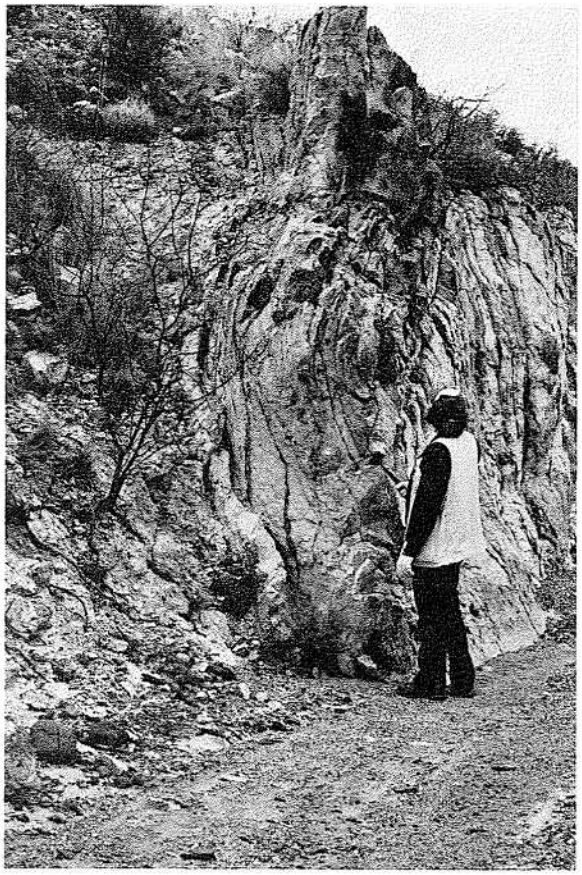

FIGURE 12. Dike of flow-banded rhyolite porphyry intruded into tuff-breccia.

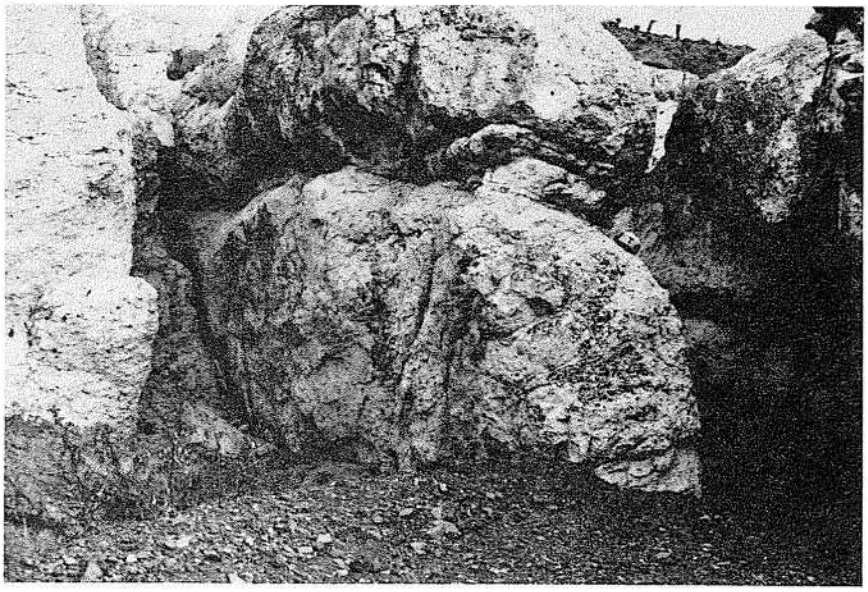

FIGURE 13. Tuff-breccia consisting of rhyolite porphyry, pumice, and pre-Tertiary rock fragments in a tuffaceous matrix.

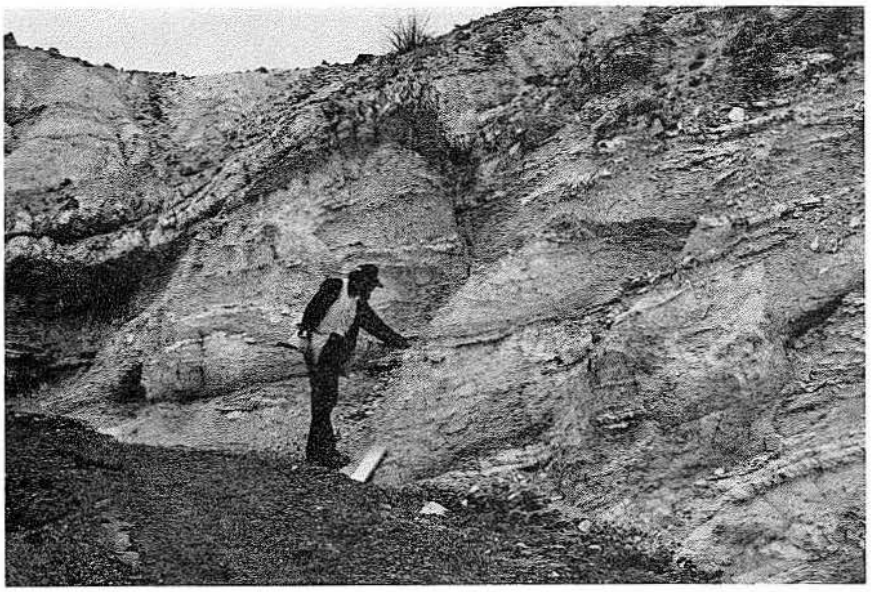

FIGURE 14a. Crudely bedded tuff-breccia, probably air-fall tuff.

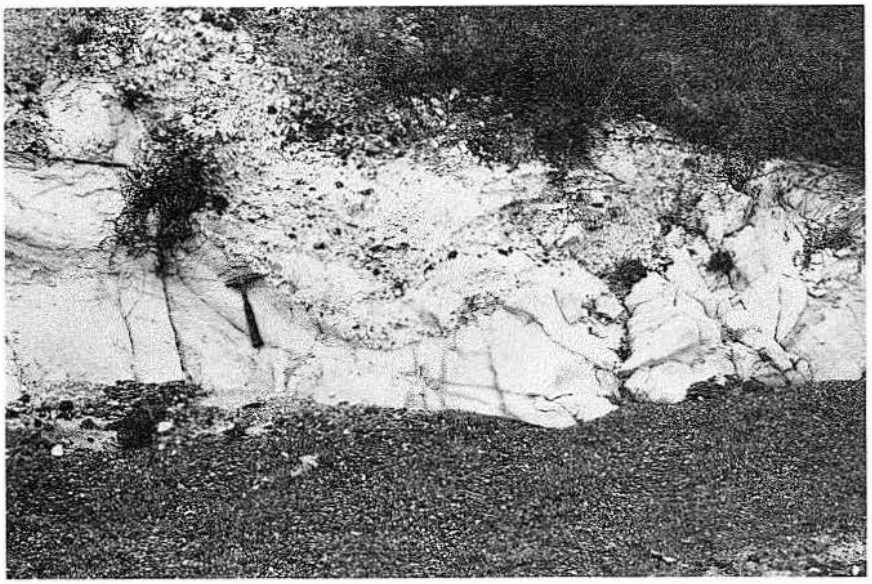

FIGURE 14b. Channel filled with water-laid tuff within tuff-breccia sequence.

and because of, caldera collapse. Precambrian rock fragments can be found throughout the caldera but are abundant only in the northwestern part. Precambrian rocks crop out just outside the northwestern caldera wall (see plate) but were probably never exposed in the wall, at least at the present level of exposure. Thus the Precambrian fragments and probably many others must have been brought up from depth by the explosive volcanism.

The highest outcrops and thus probably stratigraphically highest rocks are the least tuffaceous and generally finest grained. For example, the outcrop due south of High Lonesome Peak is composed dominantly of angular rhyolite porphyry clasts as much as 10 cm in

FIGURE 15. Extremely coarse tuff-breccia with randomly oriented blocks of Cretaceous rocks. A tuffaceous matrix crops out below the large limestone block left of person.

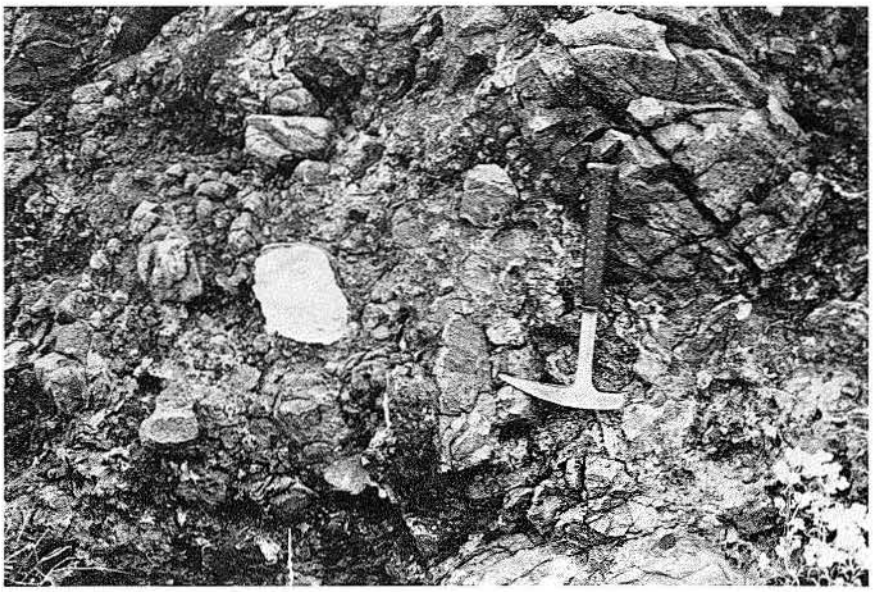

FIGURE 16. Internal brecciation of a 50-m block of Cox Sandstone within tuff-breccia.

diameter. Quartz and feldspar grains are common, but pumice fragments are minor, and most are less than 1 cm in diameter.

The tuff-breccia grades further upward into well-bedded tuffaceous sediment, containing abundant quartz, feldspar, and biotite grains as large as 1 and 2 mm in diameter. The contact between this tuffaceous sediment and the tuff-breccia is gradational and irregular. Considerable local relief must have existed on the tuff-breccia surface before deposition of the sediment. Some outcrops are only crudely bedded and share characteristics of both the tuff-breccia and the

tuffaceous sediments. The mapped contact should be considered the approximate location of a gradational change.

The tuff-breccia may have multiple origins. Parts near the rhyolite porphyry include probable debris avalanches and sedimentary deposits derived from the rhyolite. Elsewhere the tuff-breccia is certainly pyroclastic but could be either ash-flow or air-fall tuff or both. The massive, coarse, and unsorted deposits suggest ash-flow tuff. However, shards, characteristic of ash-flow tuffs, are rare or absent. Devitrification does not seem to have been sufficiently intense to destroy all shard texture. Much of the tuff-breccia may have been deposited as air-fall tuff. Heiken and Wohletz (1984) indicate that ash produced during phreatomagmatic eruptions is largely nonvesicular and consists mostly of blocky pieces of the intrusion itself. Such coarse deposits would lack the stratification characteristic of fine-grained air-fall tuff. Whatever its origin, the tuff-breccia clearly accumulated in an already existing caldera basin with well-defined walls and represents a continuation of the pyroclastic activity that generated the underlying ash-flow tuff. With time, tuffaceous activity and intrusion ceased or at least declined dramatically. Deposition gradually changed to lacustrine and fluvial sedimentation; the component of local tuffaceous material decreased.

Occurrence and distribution of the rhyolite porphyry and tuff-breccia may fit a model suggested for rhyolite dome complexes (Fink, 1983). In Fink's model, differentiation of a shallow, rhyolitic magma produces an upper phenocryst-poor and volatile-enriched zone over a lower phenocryst-enriched magma. With sufficient volatile enrichment, contact with ground water, or pressure release, the upper zone erupts to form a blanket of coarse air-fall tuff. Continued rise of the underlying magma allows intrusion of rhyolite into the air-fall tuff. The rhyolite dome can even break through to the surface to shed coarse debris off its flanks and send flows over the earlier tuff. In Fink's model, earliest flows are commonly pumiceous obsidians. Emplacement of phenocryst-rich magma is the final event. However, because the phenocryst-rich magma has a much higher viscosity than the volatile-rich, phenocryst-poor magma, it does not flow far and instead solidifies in place as a stock or dome. With the exception of obsidian flows, this model is generally consistent with the types of rocks and sequence of events in the Van Horn Mountains caldera.

Hogeye Tuff

The Hogeye Tuff is a regional unit, derived in part from tuffs erupted from the Van Horn Mountains caldera. Twiss (1959b) mapped much of the tuffaceous sediments of the Van Horn Mountains as the Hogeye Tuff. However, he also included within the Hogeye several units we have mapped separately, including the ash-flow tuff and tuff-breccia that fill the Van Horn Mountains caldera and some basaltic lava flows that are interbedded with tuffaceous sediments near the top of the Hogeye Tuff. Our subdivision of the various tuffaceous units is shown in figures 4 and 17. We have restricted the term "Hogeye Tuff" to bedded, commonly zeolitic, tuffaceous sediments that crop out both within and outside the caldera (fig. 17).

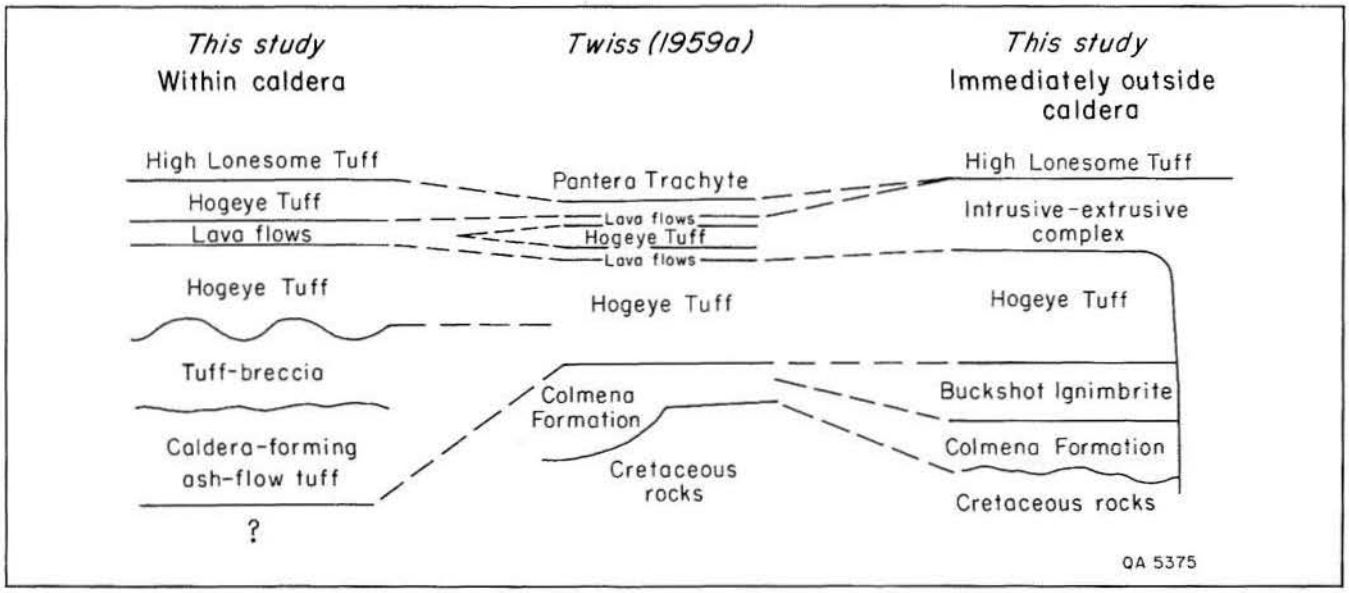

FIGURE 17. Volcanic stratigraphy within and near the Van Horn Mountains caldera. Not to scale.

The Hogeye Tuff, as we have mapped it, crops out in two locations outside the caldera: (1) near Carpenter Lodge at the southeastern margin of the caldera and (2) about 1 km northeast of the northeastern caldera margin. In the former location both the Buckshot Ignimbrite and High Lonesome Tuff are present, and the Hogeye interval is clearcut. In the latter the Buckshot is not present, and tuffaceous sediment rests directly on Cretaceous sedimentary rocks, a situation also recognized by Twiss. This section may include deposits older than the strict Hogeye interval and temporally equivalent to the Colmena Formation. However, the Buckshot at Carpenter Lodge rests directly on Cretaceous rocks, and the Colmena Formation farther to the southeast consists of limestone conglomerates distinctly unlike the tuffaceous sediments northeast of the caldera. Thus, the sediments we have mapped northeast of the caldera are probably all within the formal Hogeye interval.

Within the caldera, the Hogeye Tuff as mapped by Twiss (1959b) includes units we have identified as ash-flow tuff associated with caldera collapse and tuff-breccia that filled the caldera after collapse. We have used the term "Hogeye" to include only the bedded tuffaceous sediment interval between the tuff-breccia and the High Lonesome Tuff. As mentioned above, the contact between the tuff-breccia and the tuffaceous sediment is gradational, reflecting termination of the initial phase of explosive volcanism in the Van Horn Mountains caldera. Because both the ash-flow tuff and tuff-breccia are clearly younger than the Buckshot Ignimbrite, the Hogeye Tuff mapped within the caldera represents only the upper two-thirds of the Hogeye outside the caldera. The Buckshot Ignimbrite and the lower third of the Hogeye could occur in the downdropped caldera block beneath the ash-flow tuff.

The Hogeye Tuff is generally fine-grained, bedded tuffaceous sediment typical of similar deposits throughout Trans-Pecos Texas. The Hogeye Tuff in the Van Horn Mountains is more variable than most other deposits because parts of it were deposited within or near a caldera that was also the source of much of the tuffaceous material. Two distinct types of deposits are recognizable: (1) a coarser grained, finely laminated, probably lacustrine deposit, which makes up the lower third of the Hogeye Tuff within the caldera and all of the section near Carpenter Lodge and (2) a finer grained but more thickly bedded, probably fluvial deposit that makes up the upper two-thirds of the tuff within the caldera and all of the section in the area just northeast of the caldera.

The lower "lacustrine" part is commonly finely laminated and shows distinctive sedimentary features, including ripple marks and minor crossbedding. Individual laminae are as little as 0.5 mm thick. The overall appearance suggests lacustrine deposition (Picard and High, 1972), which would be consistent with accumulation in the closed caldera basin.

Detrital grains include coarse (up to 4 mm in diameter) quartz, biotite, and porphyritic rock fragments clearly derived from local sources, either (1) by reworking of the ash-flow tuff, rhyolite porphyry, or tuff-breccia or (2) by continued infusion of air-fall material. The groundmass contains abundant pumice and glass shards.

The upper "fluvial" part of the Hogeye Tuff is thinly bedded but otherwise structureless (fig. 18); it is similar to the more regional tuffaceous sediments of Trans-

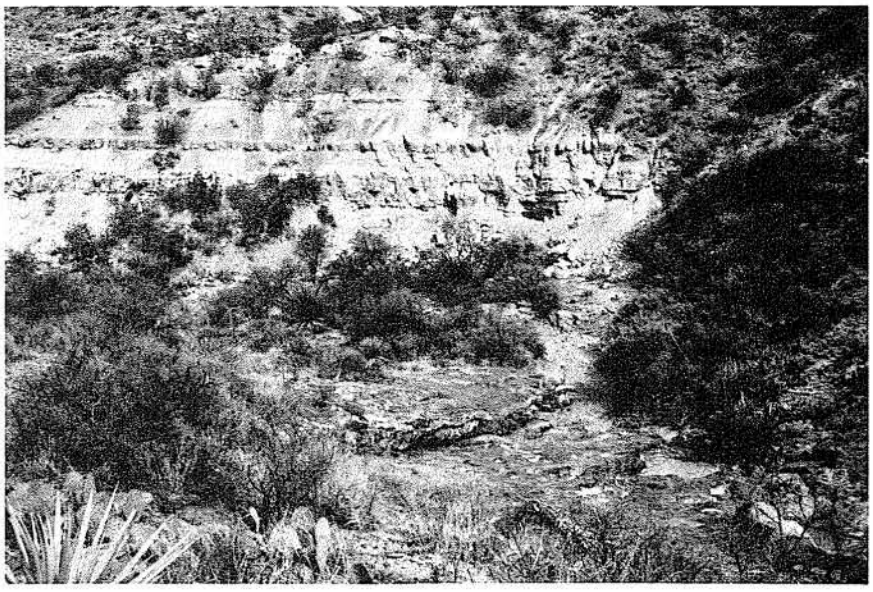

FIGURE 18. Fluvial tuffaceous sediments in the Hogeye Tuff.

Pecos Texas, such as those of the Vieja Group. Individual beds are several centimeters to several tens of centimeters thick. Except for the clearly detrital nature of component grains and rare crossbedding, sorting, or other sedimentary features, the tuff could be considered air fall in origin. However, Walton (1975) has demonstrated that similar deposits in the Vieja Group are fluvial sediments. Detrital grains include fine (<1 mm) quartz, feldspar, pumice, and glass shards; biotite is absent or very minor and is about 0.25 mm in diameter.

All of the Hogeye Tuff has been diagenetically altered and is well indurated. Clinoptilolite and minor montmorillonite fill spaces left by dissolution of glass and generally cement the rock. In addition, some lacustrine deposits and the lower part of the tuff near Carpenter Lodge are intensely silicified.

Thickness of the Hogeye Tuff ranges up to 57 m on the north face of High Lonesome Peak (Twiss, 1959a). Twiss also measured 32 m of tuffaceous sediment on the south face of High Lonesome Peak. This latter section extends up from a hill of tuff-breccia, which was probably a topographic high at the time of deposition. The Hogeye outside the caldera is thinner, estimated at 20 m northeast of the caldera and 12 m near Carpenter Lodge.

Intrusive-Extrusive Complex

An intrusive-extrusive complex, dominantly composed of basalt and trachyte but including some rhyolite, was emplaced just outside the eastern margin of the caldera (see plate). The intrusive source is in contact only with Cretaceous rocks; thus an age relative to other igneous rocks cannot be determined. However, flows to the north and west either directly underlie the High Lonesome Tuff or are interbedded with tuffaceous sediments of the Hogeye Tuff below the High Lonesome Tuff.

Field Relations

We have subdivided the complex into (1) a central intrusive part composed dominantly of trachyte but including a small rhyolite dome and a basaltic vent and (2) outlying lava flows, composed dominantly of basalt with lesser trachyte and minor rhyolite. Identification of the outlying flows from field relations is simple, but delineation of the central intrusive part is less straightforward. The mapped intrusive area probably includes some flows. Cretaceous rocks dip away from the intrusion, indicating doming, in several places along its western margin. In other places, the contact is flat, and Cretaceous rocks are flat lying up to the contact (fig. 19a). In these locations the intrusion may have been laccolithic or emplaced passively; alternatively, parts may be extrusive. However, no basal flow breccias are exposed along the contact, although they are common at the base of definite flows. Near the center of the intrusive area, trachyte crops out in several concentric, vertical bands, about 10 m wide separated by poorly exposed tuffaceous material (fig. 19b). This relationship suggests intrusion through the tuff. Finally, a small intrusion southwest of the main area has vertical contacts with surrounding rocks, including the Garden of the Gods intrusion, and is undoubtedly intrusive.

Trachyte composes most of the main intrusion. However, a rhyolite dome intrudes the trachyte, and a basaltic agglomerate may mark a former vent. The rhyolite is nearly circular and about 150 m in diameter; flow banding dips gently outward on all sides. The agglomerate is about 200 m by 400 m and consists of coarse, angular to rounded blocks of basalt in an ashy matrix. The dome and agglomerate may mark source areas of, respectively, rhyolitic and basaltic flows that crop out to the west within the caldera.

Hogeye Tuff and High Lonesome Tuff overlie the central intrusive area and demonstrate that it was emplaced at a shallow depth and rapidly unroofed. We envision a shallow stock feeding flows that extended from the stock. Minor dikes of basalt, trachyte, and rhyolite within and near the caldera could have been additional sources for the flows.

Basaltic, trachytic, and minor rhyolitic lava flows extended from the central intrusive area to the north, south, and west. Basaltic flows spread farther than trachytic or rhyolitic flows, which occur only within about 2 km of the intrusive source. To the north, lavas flowed down a valley cut in Cretaceous rocks and already partly filled with Hogeye Tuff. The northern contact between intrusive and extrusive parts is speculative. To the south, basaltic flows directly overlie Cretaceous rocks and are not in contact with other volcanic rocks. Twiss (1959b) mapped these lava flows as part of the Colmena Formation. We combine them with the intrusive-extrusive complex on the basis of petrographic and chemical similarities, but stratigraphic control is lacking. To the west, lavas overlapped the caldera rim and flowed down into the caldera. At and near the margin, several flows of basalt and trachyte are interbedded with Hogeye Tuff. More distant outcrops are dominantly basalt, which is exposed irregularly across the western part of the caldera but may have been more continuous at the time of deposition. A basalt flow crops out 5 to 10 m below the High Lonesome Tuff around High Lonesome Peak except where concealed by colluvium.

Rhyolites are minor but include more than the three small outcrops shown on the plate. A thin, flow-banded rhyolite commonly having a glassy base underlies basalt in several hills in the south-central part of the caldera. Generally these outcrops are too thin to show

FIGURE 19a. Hill of intrusive trachyte (background) cut into gently dipping Cretaceous rocks (left and in valley in middle).

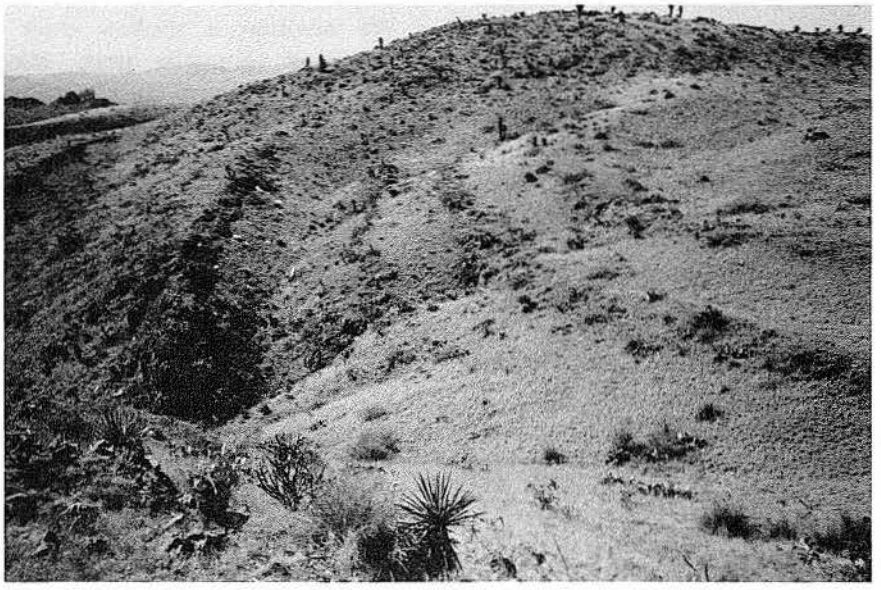

FIGURE 19b. Concentric, vertical bands of resistant trachyte and nonresistant tuff within the intrusive-extrusive complex. The trachyte was apparently intruded through tuff. Flat-lying tuffaceous sediments of the Hogeye Tuff and High Lonesome Tuff overlie trachyte in the hill in the background.

on the plate, except for the outcrop represented by sample 81-206. At that sample location, the overlying basalt has been eroded, leaving the hill capped by flow-banded rhyolite. In outcrop, the rock appears to be a lava flow, but thin sections of vitrophyre show a flattened-shard texture, suggesting an ash-flow tuff. The flow may have been derived from a small rhyolite intrusion ½ km northwest of Carpenter Lodge (see plate) or from the central intrusive complex. The distribution of the different lava flows is probably a

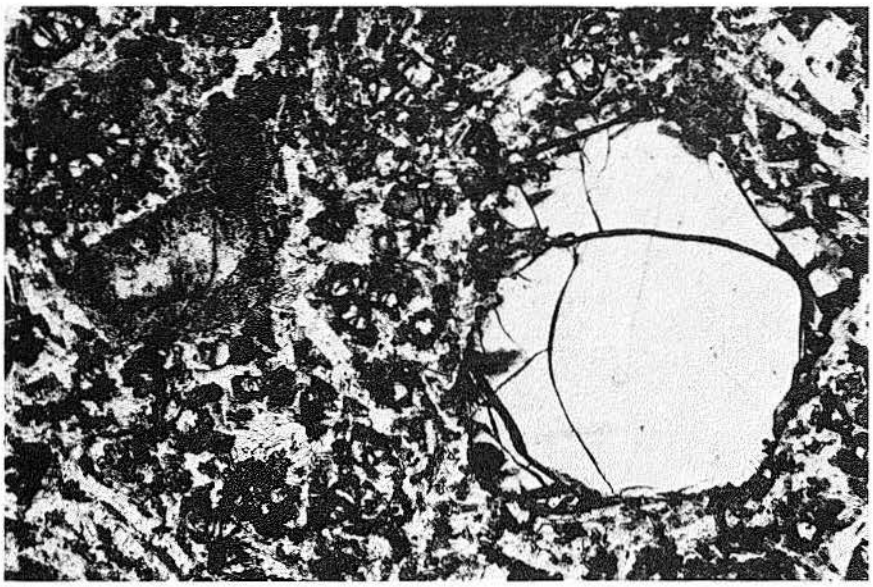

FIGURE 20. Photomicrograph of basalt with olivine and clinopyroxene phenocrysts in groundmass of plagioclase, olivine, clinopyroxene, and magnetite. Long dimension is 3.6 mm.

function of source location and magma viscosity. Low-viscosity basalts could flow the farthest so are most widely distributed. Higher viscosity trachytes could not flow as far so occur only near or within the intrusive center. Rhyolites should be similarly restricted; their somewhat wider distribution than the trachytes suggests additional sources.

Petrography

Basalts contain olivine (FO_{85}) and plagioclase phenocrysts in addition to pinkish-gray clinopyroxene (fig. 20). The olivine is commonly fractured and altered to serpentine, iddingsite, and goethite. In one sample the clinopyroxene had unaltered cores with "worm-eaten" margins consisting of clinopyroxene and iron-titanium oxides. The groundmass consists of plagioclase, olivine, clinopyroxene, apatite, magnetite, and ilmenite-hematite. Minor patches of chlorite may be alteration products of interstitial glass.

Trachytes contain phenocrysts of a nearly colorless clinopyroxene, orthopyroxene, sanidine-anorthoclase, and iron-titanium oxides (fig. 21). The pyroxenes commonly occur as glomerocrysts and are altered to mosaics of calcite and chlorite. The groundmass consists of feldspar microlites, clinopyroxene, magnetite, and ilmenite-hematite.

The rhyolite flow is highly vesicular and commonly contains sparse quartz and biotite phenocrysts. The groundmass consists of alkali feldspar microlites, opaques, and an irregular brown material that may be devitrified glass. Minor opal and possible zeolites line vesicles. The rhyolite flow contains small (<0.5 mm) phenocrysts of alkali feldspar, clinopyroxene, opaques, and zircon. A sample of vitrophyre has a groundmass of highly flattened shards, although broad, continuous flow bands indicative of a lava flow extend through the rock.

High Lonesome Tuff

The High Lonesome Tuff is a 37- to 38-m.y.-old (table 3, p. 38) rhyolitic ash-flow tuff, whose probable source is the Van Horn Mountains caldera. It was originally called the Pantera Trachyte by Twiss (1959a) and correlated with the Pantera Trachyte of the Wylie Mountains mapped by Hay-Roe (1957); this usage was continued by Barnes (1979) in the Marfa sheet of the Geologic Atlas of Texas. For the following reasons, we propose to formally rename part of the Pantera Trachyte of Twiss the High Lonesome Tuff and to restrict the name Pantera Trachyte to the appropriate lava flows of the Wylie and Van Horn Mountains. The new name is derived from excellent, thick exposures on High Lonesome Peak (fig. 22). The type section is from Twiss' (1959b) measured section 10 on the north side of the peak; the High Lonesome Tuff exactly corresponds to his Pantera Trachyte.

The Pantera Trachyte was initially recognized and mapped by Hay-Roe (1957) in the Wylie Mountains to

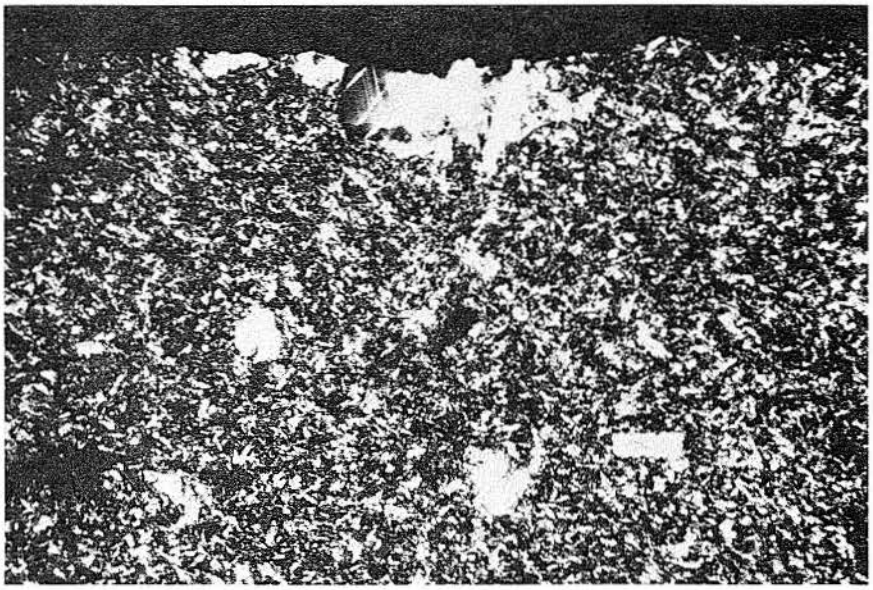

FIGURE 21. Photomicrograph of trachyte with clinopyroxene and plagioclase phenocrysts in groundmass of plagioclase, clinopyroxene, magnetite, and ilmenite-hematite. Long dimension is 3.6 mm.

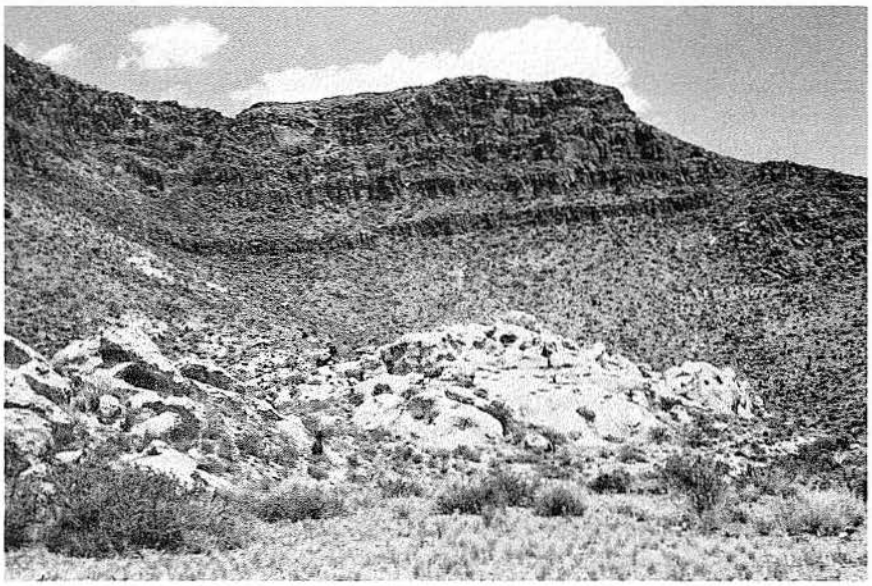

FIGURE 22. Thick High Lonesome Tuff composed of at least five separate ash flows capping a ridge and overlying the Hogeye Tuff. The massive outcrop in the foreground is tuff-breccia.

the east across the basin of Lobo Valley, where it is dominantly a series of lava flows. In his mapping, Twiss (1959a) recognized the distinction but, because the rocks occupied a similar stratigraphic position and were petrographically similar, decided that the two rock types were related. He concluded that the lava flow may have been a rheoignimbrite. Teal and Hoffer (1980) incorrectly identified the Pantera Trachyte in the Wylie Mountains as an ash-flow tuff. The work of Twiss and our work show conclusively that the "Pantera" in

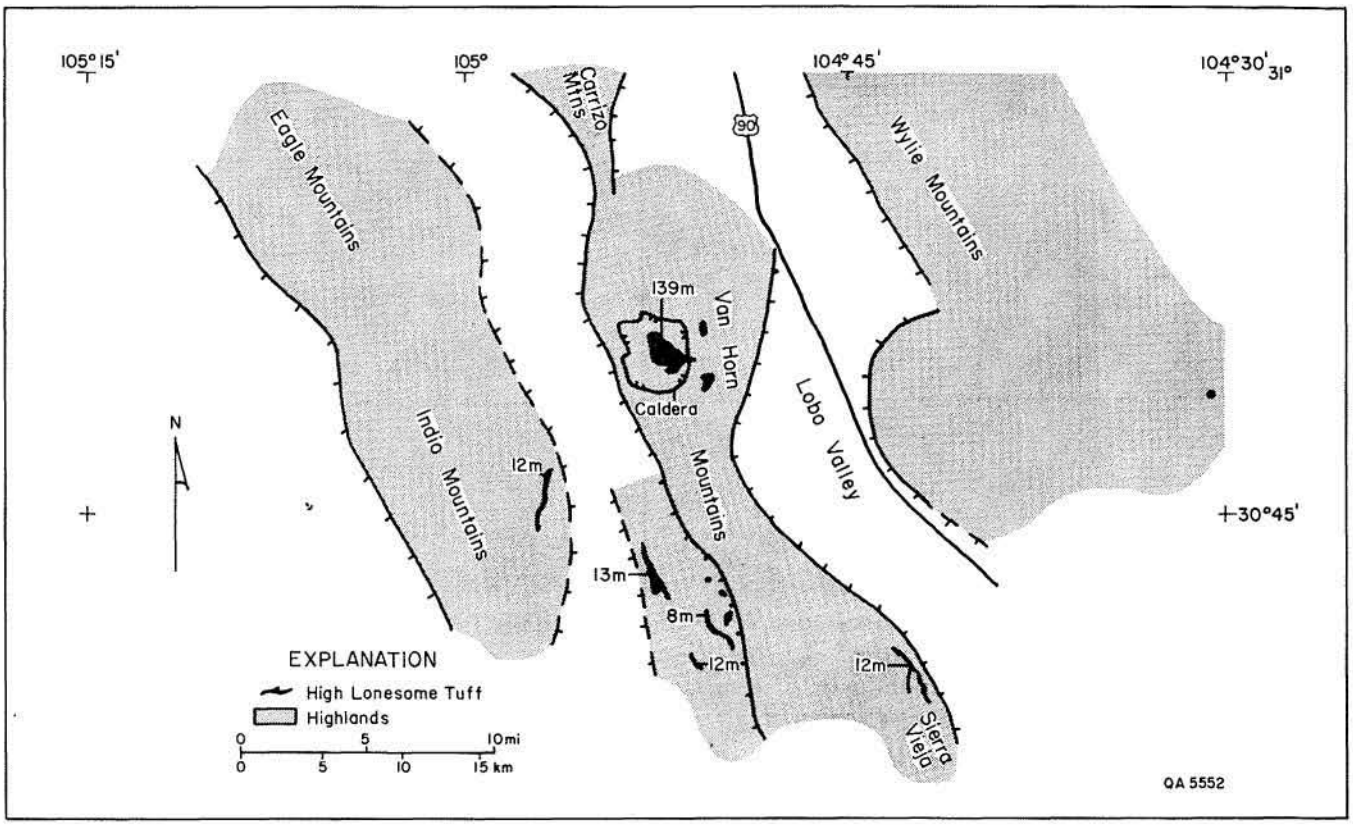

FIGURE 23. Known distribution of High Lonesome Tuff. Measured thicknesses in meters are from Twiss (1959a). Additional outcrops probably occur in the Wylie Mountains.

the Van Horn Mountains and in nearby areas to the southwest and south is an ash-flow tuff. Pantera Trachyte as mapped by Twiss (1959b) in the northeastern Van Horn Mountains is dominantly a series of lava flows and is probably correlative with the Pantera Trachyte in the Wylie Mountains. Some "Pantera" ash-flow tuff (High Lonesome Tuff) does occur in the Wylie Mountains (T. W. Duex, personal communication, 1980) but is minor. Identification of its complete distribution in the Wylie Mountains awaits further mapping.

Figure 23 shows the known distribution of the High Lonesome Tuff. Although the Van Horn Mountains caldera is probably the source of the tuff, eruption of the High Lonesome Tuff was not responsible for initial caldera collapse; the tuff simply ponded within the pre-existing caldera. It is as much as 139 m thick within the caldera, as measured at its type locality (see plate) on the slopes of High Lonesome Peak (Twiss, 1959a). Outside the caldera it is much thinner; a typical thickness is 12 m in sections measured in the Indio Mountains, the southern Van Horn Mountains, and the northern Sierra Vieja (Twiss, 1959a; Underwood, 1963). It pinches out in the northern Sierra Vieja. The High Lonesome Tuff may also have extended to the north and west, symmetrically around the caldera, and later eroded, although volume considerations indicate that it cannot have been extensive.

Estimated volume of the High Lonesome Tuff includes about 1 km^3 of caldera fill and 2 to 10 km^3 of outflow. This estimate of caldera fill assumes an average thickness of 100 m over the 10 km^2 area of the caldera. The low estimate of outflow tuff volume assumes that it spread primarily to the south. On the basis of the size of the caldera, discussed below, the low estimate is realistic; greater volumes are unlikely.

The tuff is densely welded everywhere observed, including both the thick outcrops within the caldera and thinner outcrops outside the caldera. Within the caldera it consists of numerous ash flows. Distinct layering, consisting of benches within the ash-flow tuff, suggests at least five ash flows or minor cooling breaks at the base of High Lonesome Peak (fig. 22). Major cooling breaks are not present, but we have not made a detailed study to identify minor breaks within the caldera. Immediately outside the caldera along the ridge extending east-southeast from High Lonesome

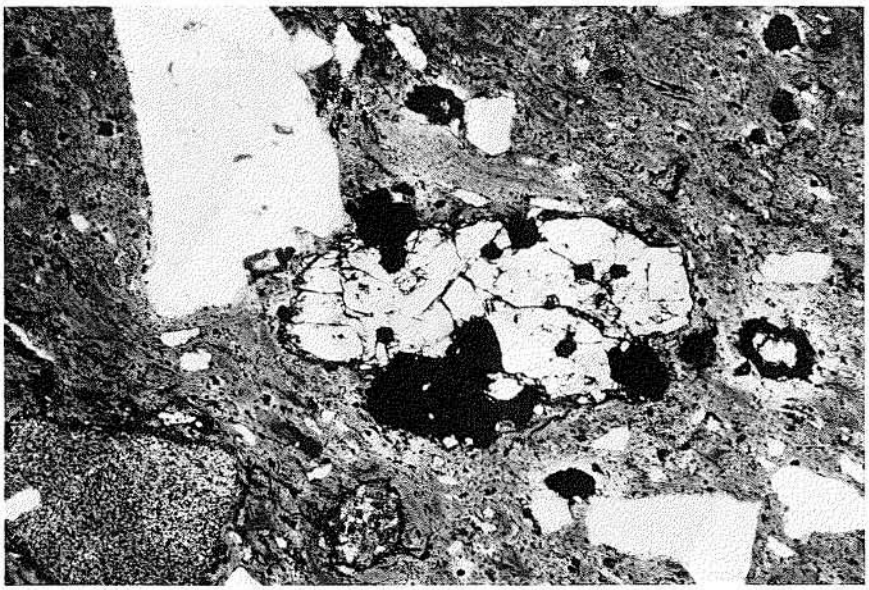

FIGURE 24. Photomicrograph of High Lonesome Tuff vitrophyre with phenocrysts of alkali feldspar, clinopyroxene, and various opaque minerals in groundmass of compacted glass shards. Long dimension is 3.6 mm (uncrossed nicols).

Peak, cooling breaks are more obvious. We interpret individual cooling units to represent single ash flows. The lowest flow has a perlitic, gray vitrophyre overlain by a poorly welded, devitrified zone. A second flow, overlying the first, has a black vitrophyre with a densely welded, devitrified zone above it. An outcrop more distant from the caldera in the southern Van Horn Mountains consists of four ash-flow units with a cooling break between each. Hydrated vitrophyre occurs at the base of the lowest two ash flows. Further to the south in the northern Sierra Vieja, we have recognized only one flow, but it is possible that welding, devitrification, and vapor-phase crystallization have obscured flow boundaries. Hydrated vitrophyres are exposed at the base of the High Lonesome Tuff in many locations both within and outside the caldera. Vitrophyre may be present over most of its outcrop, but talus commonly covers the base.

The High Lonesome Tuff contains 6 to 12 percent alkali feldspar phenocrysts in a groundmass of glassy or devitrified shards. Plagioclase is a minor constituent in some samples; two clinopyroxenes, a nearly colorless pigeonite and a pleochroic brownish-green augite, were probably present initially in all rocks but are preserved only in vitrophyres. Oxidation during devitrification has converted clinopyroxenes and any other mafic minerals to iron oxides. Titanomagnetite phenocrysts have been oxidized to oriented intergrowths of ilmenite and hematite. Primary ilmenite phenocrysts appear to be unoxidized. A pyrrhotite inclusion was noted within a clinopyroxene phenocryst of a vitrophyre (fig. 24). Small rock and pumice fragments make up at most a few percent of some samples.

Although the major part of the Van Horn Mountains caldera formed earlier, additional subsidence may have occurred during emplacement of the High Lonesome Tuff. The tuff dips gently inward from all directions toward High Lonesome Peak. This attitude is most pronounced along the ridge east of the peak; although much of the base is covered by landslide debris, it clearly drops from ~1,650 m near the inferred eastern caldera edge to less than 1,460 m due north of High Lonesome Peak. The dip of the tuff may have resulted from general subsidence of the central or western part of the caldera without actual slip along caldera faults. Alternatively, the tuff may have simply filled in against wedge-shaped topography developed on trachyte that spilled into the caldera from its source to the east.

The High Lonesome Tuff must have nearly filled the caldera because ash flows along the eastern rim spilled over and flowed down the north-trending valley occupied by lava flows of the intrusive-extrusive complex. The tuff is exposed along this trend only as discontinuous remnants directly on top of the lavas.

Tuffaceous Sediments Above the High Lonesome Tuff

A 25-m-thick sequence of coarse sandstones and conglomerates (Twiss, 1959a) overlies the High Lonesome Tuff on High Lonesome Peak. Angular, poorly sorted volcanic rock fragments as much as 4 cm in diameter (including many from the underlying ash-flow tuff), alkali feldspar grains, and pumice fragments as much as 1 cm in diameter make up the framework. The sediments are poorly indurated and friable probably because the low glass content did not allow for extensive cementation during diagenesis. Coarseness of the deposits and the minor tuffaceous component indicate that the sediments accumulated within the caldera basin at the end of pyroclastic activity and from entirely local sources.

A tuffaceous interval also overlies the High Lonesome Tuff in the Indio Mountains and in the Colquitt Syncline in the southern Van Horn Mountains (Twiss, 1959b). However, these tuffaceous sediments are similar to the regional deposits of the area; that is, they are finer grained, more tuffaceous, and consequently more zeolitic than the sediments on High Lonesome Peak. Although some of the material in these other deposits may have been derived from the Van Horn Mountains caldera, their dominant source probably was elsewhere.

Trachyte of High Lonesome Peak

A series of trachyte lava flows, the youngest volcanic rocks in the area, overlie the tuffaceous sediments on High Lonesome Peak. The trachyte is aphanitic to very sparsely porphyritic and contains 1 percent normally zoned plagioclase phenocrysts as long as 3 mm. The light-gray groundmass is made up of very fine trachytic alkali feldspar. A basal breccia occurs on High Lonesome Peak, and in places the lava flows are vesicular with chalcedonic fillings. However, poor exposure of the units precludes determining the number of flows present. Twiss (1959a) measured a thickness of 93 m.

Twiss (1959a) correlated these flows with trachytes in a similar stratigraphic position to the west, along Green River, and to the south, in the Indio Mountains and in the Colquitt Syncline. The trachyte in both these areas is similar, although flows to the west contain about 5 percent phenocrysts. Neither these flows nor the flows on High Lonesome Peak correlate with the coarsely porphyritic Pantera Trachyte lava flows of the northeastern Van Horn Mountains or the Wylie Mountains.

The source of these late trachyte flows and their genetic relation to the Van Horn Mountains caldera are not certain from field evidence. They are petrographically similar to the trachytes underlying the High Lonesome Tuff, but the general rock type is common throughout Trans-Pecos Texas. Clearly the flows were once more extensive and probably covered the caldera.

Miocene to Recent Basin Fill

Poorly consolidated conglomerate, sandstone, and siltstone occupy the Basin and Range basins of Green River Valley and Lobo Valley to the west and east of the Van Horn Mountains. They were derived from erosion of the older rocks of the area and were deposited as alluvial fans and lacustrine sediments in the initially closed basins. Integration of the Rio Grande in Pleistocene time has allowed dissection of the western basin. The eastern basin is still part of a closed drainage system, although the base level is in Salt Basin, more than 50 km to the north. Strictly speaking, alluvium currently being deposited in either basin is still basin fill.

Quaternary Deposits Within the Van Horn Mountains Caldera

Quaternary terrace deposits, alluvium, and landslide deposits are the youngest rocks in the area. A thin gravel terrace covers bedrock in the central part of the caldera; small, unmapped remnants cap ridges in the western part. A cap of such deposits probably once covered all the present lowlands in the western part of the caldera but has been largely removed by downcutting of the creek that drains that area. Two major landslide blocks occur northeast and east of High Lonesome Peak where massive High Lonesome Tuff slid on softer Hogeye Tuff sediments.

GEOCHEMISTRY

The rocks of the Van Horn Mountains caldera and vicinity are alkali-calcic by the classification of Peacock (1931). They are geochemically similar to rocks of other volcanic centers of the western metaluminous (Barker, 1979) or alkali-calcic (Henry and Price, 1984) belt of Trans-Pecos Texas. They are relatively alkali rich and range in composition from basalt (hawaiite) to trachyte to rhyolite (see table 1, which also lists CIPW norms). Figures 25, 26, 27, and 28 show plots of various oxide and element components using volatile(H_2O and CO_2)-free compositions. All discussions of the trends are based on volatile-free compositions. The appendix provides petrographic descriptions of analyzed or dated samples. This initial study reports the data and briefly discusses their significance. A more detailed petrologic study is underway.

TABLE 1. Chemical analyses of rocks from the Van Horn Mountains caldera.

	Precollapse rhyolite	Caldera-forming ash-flow tuff	Rhyolite porphyry			Hogeye Tuff	Intrusive-extrusive complex					
	81-119	H84-13	81-118	81-207	81-214	81-186	81-206	81-120	82-91	82-90	81-196	82-89
Major oxides (weight percent)												
SiO_2	73.55	75.35	79.55	78.13	76.12	73.78	76.11	71.91	60.11	59.25	59.98	58.64
TiO_2	0.08	0.09	0.08	0.07	0.07	0.39	0.04	0.25	1.03	1.05	1.02	1.57
Al_2O_3	13.35	12.30	13.08	12.12	12.27	13.17	12.25	13.71	14.53	14.55	14.67	14.22
Fe_2O_3	1.64	<0.01	<0.01	0.08	0.23	1.69	0.38	1.77	5.15	5.25	4.40	1.93
FeO	0.17	1.08	0.15	0.24	0.37	0.51	0.53	0.06	1.22	1.14	1.68	5.66
MnO	0.03	0.01	0.04	0.01	0.02	0.03	0.05	0.06	0.11	0.10	0.13	0.15
MgO	0.15	0.14	0.08	0.05	0.06	0.67	0.09	0.12	3.34	3.76	3.12	2.82
CaO	0.85	2.30	0.19	0.43	0.35	0.73	0.64	0.71	5.54	6.56	5.91	4.34
Na_2O	3.88	1.06	1.39	1.93	1.36	1.87	3.65	2.83	3.66	3.67	3.73	3.71
K_2O	5.11	4.70	4.92	6.49	7.40	5.88	5.18	7.48	4.07	2.98	3.68	3.44
P_2O_5	<0.01	<0.25	<0.01	<0.06	<0.06	<0.06	<0.06	0.07	0.26	0.28	0.31	0.65
CO_2	0.50	<0.15	<0.05	0.21	0.39	0.32	0.32	0.13	0.53	1.47	0.65	2.61
H_2O^+	0.59	3.99	0.92	0.32	0.76	0.57	0.30	0.17	0.42	0.54	0.53	0.15
Total	99.90	101.05	100.40	100.08	99.40	99.61	99.54	99.27	99.97	100.60	99.81	99.89
Trace elements (ppm)												
Be	8	—	2	<1	1	<2.5	9	4	—	—	<2.5	—
F	210	—	240	190	240	1,340	460	260	—	—	530	860
V	7	—	3	<5	<5	<25	<5	24	—	—	130	—
Cr	<1	—	4	<10	<10	13	<10	20	—	—	160	—
Ni	<2.5	—	<2.5	<10	<10	<25	<10	11	—	—	64	—
Cu	9	—	2	4	4	<10	4	7	—	—	26	—
Zn	120	<40	9	8	58	62	57	45	58	57	74	97
Rb	315	—	—	317	425	235	341	250	—	—	143	—
Sr	26	266	38	49	46	75	13	50	435	489	435	322
Y	73	—	—	19	29	46	56	28	—	—	30	—
Zr	195	—	55	59	62	268	64	71	<40	<40	128	97
Nb	63	—	—	8	10	34	93	27	—	—	29	—
Mo	2.9	—	1.4	4.0	17	3.0	3.4	1.8	—	—	1.5	—
Ba	25	134	68	105	93	365	29	306	840	374	397	688
Norms (weight percent)												
q	30.75	46.15	52.01	41.52	39.62	38.71	34.11	25.68	11.00	13.15	11.86	16.40
c	1.05	2.08	5.12	1.63	2.02	3.14	0.22	0.14				4.11
or	30.19	27.77	29.07	38.35	43.72	34.74	30.61	44.19	24.05	17.61	21.74	20.32
ab	32.83	8.97	11.76	16.33	11.51	15.82	30.89	23.95	30.97	31.06	31.56	31.39
an	1.06	9.26	0.94	0.81		1.60	1.15	2.24	11.20	14.43	12.42	0.78
ne												
di									8.75	5.44	8.38	
hy	0.37	2.20	0.42	0.40	0.56	1.67	0.91	0.30	4.26	6.84	3.89	13.51
ol												
mt	0.41			0.12	0.33	0.61	0.55		1.31	0.96	2.88	2.80
il	0.15	0.17	0.15	0.13	0.13	0.74	0.08	0.26	1.96	1.99	1.94	2.98
hm	1.35					1.27		1.77	4.25	4.59	2.41	
ru								0.12				
ap								0.15	0.57	0.61	0.68	1.42
cc	1.14	0.77		0.48	0.62	0.73	0.73	0.30	1.21	3.34	1.48	5.94

— = Not analyzed.

All analyses made after heating to 110°C for 24 hr to drive off adsorbed water.

Analyses by inductively coupled argon plasma spectrometer:

SiO_2, TiO_2, Al_2O_3, total Fe, MnO, MgO, CaO, Na_2O, K_2O, P_2O_5, Be, Sr, Ba, Zr, Cu, Zn, V, Cr, and Ni.

CO_2 and H_2O^+ by thermogravimetric analysis and CHN analyzer.

TABLE 1 (cont.)

Intrusive-extrusive complex (cont.)							High Lonesome Tuff				Late trachyte	
81-197	82-92	81-200	H84-8	81-192	H84-10	H84-12	81-117	81-116	81-115	81-191b	81-113	
Major oxides (weight percent)												
57.13	47.93	47.81	47.57	47.06	46.80	46.69	68.65	72.14	70.45	72.24	64.21	SiO_2
0.98	3.53	1.83	2.62	2.27	3.59	3.57	0.46	0.56	0.53	0.44	0.85	TiO_2
14.11	16.96	14.75	15.84	13.89	16.32	16.29	13.33	13.34	13.97	12.55	17.22	Al_2O_3
4.73	4.76	6.53	4.48	4.97	4.47	3.55	1.01	4.04	3.20	2.81	4.00	Fe_2O_3
1.15	7.56	4.95	7.57	7.80	7.50	8.29	1.88	<0.05	0.08	0.30	0.17	FeO
0.13	0.17	0.19	0.18	0.20	0.17	0.17	0.09	0.09	0.02	0.02	0.03	MnO
2.87	5.62	7.74	6.14	9.19	5.52	5.59	0.50	0.18	0.27	0.26	0.45	MgO
6.83	8.01	9.12	7.87	9.44	7.86	7.72	1.65	0.74	0.92	0.96	2.24	CaO
2.97	3.61	3.62	3.93	2.88	3.65	4.23	3.40	3.75	3.87	2.57	5.12	Na_2O
5.36	1.55	0.96	1.39	1.18	1.94	1.81	5.51	5.12	5.26	6.87	4.70	K_2O
0.31	0.60	0.78	0.45	0.56	0.63	0.60	0.08	0.12	0.12	0.08	0.34	P_2O_5
2.57	0.15	0.46	<0.15	0.12	0.13	0.18	0.20	<0.05	0.17	0.32	0.07	CO_2
0.58	0.50	1.14	1.13	0.58	0.95	1.30	2.96	0.22	0.50	0.55	0.50	H_2O^+
99.72	100.95	99.88	99.29	100.14	99.53	99.97	99.72	100.30	99.36	99.97	99.90	Total
Trace elements (ppm)												
<2.5	—	2	—	2	—	—	5	3	4	3	3	Be
510	1,010	510	—	470	—	—	850	380	310	280	750	F
140	—	240	—	250	—	—	5	7	12	—	14	V
150	—	240	—	540	—	—	2	1	14	—	25	Cr
59	—	110	—	150	—	—	3	3	3	—	3	Ni
31	—	58	—	32	—	—	2	10	3	—	2	Cu
64	93	109	102	140	73	82	100	97	97	49	133	Zn
183	—	13	—	24	—	—	286	155	167	—	131	Rb
337	1,030	817	778	623	1,120	1,060	87	119	114	102	458	Sr
23	—	31	—	26	—	—	66	72	67	—	48	Y
134	—	173	—	236	—	—	496	521	508	530	441	Zr
28	—	18	—	28	—	—	48	60	57	—	52	Nb
1.0	—	<1	—	1.2	—	—	2.4	3.2	4.0	1.0	3.4	Mo
495	561	765	480	380	700	560	596	857	845	675	1,550	Ba
Norms (weight percent)												
9.67							23.69	29.22	26.24	29.66	12.12	q
								0.57	0.92	0.08	0.61	c
31.67	9.16	5.67	8.21	6.97	11.46	10.69	32.56	30.25	31.08	40.59	27.77	or
25.13	30.55	30.63	31.91	24.37	29.92	28.20	28.77	31.73	32.75	21.75	43.33	ab
9.34	25.50	21.16	21.48	21.49	22.42	20.12	4.84	2.89	2.71	2.22	8.45	an
			0.73		0.52	4.11						ne
4.88	7.50	12.59	11.78	16.73	9.32	10.62	1.31					di
4.89	6.20	9.22		4.67			2.61	0.45	0.67	0.65	1.12	hy
	6.20	3.67	11.42	12.24	9.88	11.22						ol
1.29	6.90	9.47	6.50	7.21	6.48	5.15	1.46					mt
1.86	6.70	3.48	4.98	4.31	6.82	6.78	0.87	0.19	0.21	0.68	0.42	il
3.84								4.04	3.20	2.81	4.00	hm
								0.46	0.42	0.08	0.63	ru
0.68	1.31	1.70	0.98	1.22	1.38	1.31	0.17	0.26	0.26	0.17	0.74	ap
5.84	0.34	1.05		0.27	0.30	0.41	0.45		0.39	0.73	0.16	cc

FeO by colorimetric oxidation-titration; F by ion-selective electrode; Mo by spectrophotometry; and Rb, Y, and Nb by X-ray fluorescence, done by Emil Bramson. All other analyses by Mineral Studies Laboratory, Bureau of Economic Geology, Dr. Clara L. Ho, director.

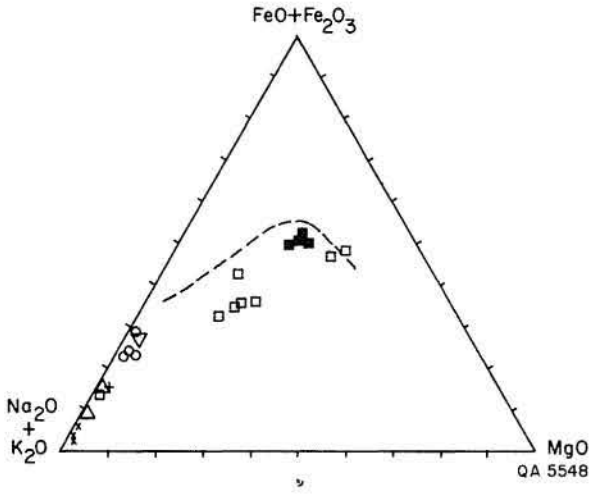

EXPLANATION

- ▽ Late trachyte
- o High Lonesome Tuff
- □ Intrusive-extrusive complex
- ■ Samples 82-92, H 84-8, H 84-10, H 84-12
- x Rhyolite porphyry
- \+ Caldera-forming ash-flow tuff
- △ Precollapse rhyolite

FIGURE 25. AFM (total alkalis, iron as FeO, and MgO) plot of rocks from the Van Horn Mountains caldera. Dashed line shows boundary of calc-alkaline (CA) and tholeiitic fields from Irvine and Baragar (1971).

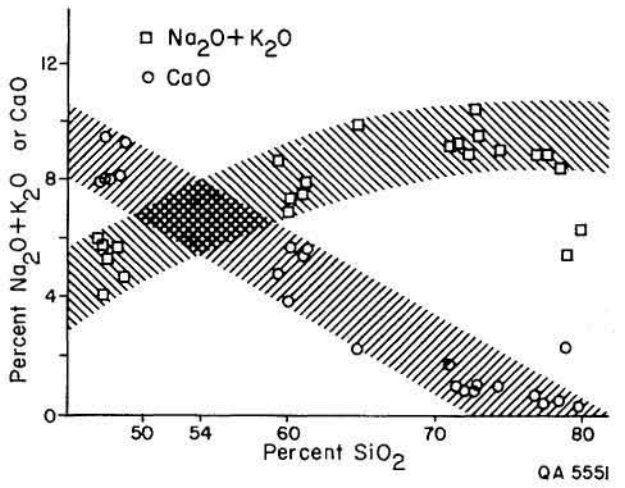

FIGURE 26. Harker variation diagram of total alkalis and CaO plotted against SiO_2. SiO_2 concentration at which total alkalis equal CaO is about 54 percent; that is, the rocks are alkali-calcic by the classification of Peacock (1931). CaO concentrations of several samples with approximately 60 percent SiO_2 are corrected for high CO_2 concentrations.

The samples were collected to be representative both of rock compositions of the caldera and of original magma compositions. In general, the first goal was easily attained. The analyzed samples include a spectrum of caldera-related rocks. Attaining the second goal was more difficult, but unaltered samples were found for most of the major rock types. Only a small part of the caldera-forming ash-flow tuff is exposed. The one sample judged suitable for analysis is hydrated and possibly silicified and has lost some sodium. Most samples of trachyte are variably altered. All but sample 82-89 are oxidized, and several samples have significant amounts of introduced calcite (appendix). At least two of the rhyolite porphyry samples (81-118 and 81-207) are silicified, and all three apparently have lost sodium and gained potassium. The four samples of High Lonesome Tuff include one hydrated vitrophyre and three devitrified rocks. FeO, Fe_2O_3, and several trace elements in the vitrophyre and SiO_2, MgO, CaO, and H_2O in the devitrified rocks are probably most representative of magmatic compositions. Finally, sample 81-186 is diagenetically altered tuffaceous sediment. Its composition is certainly not magmatic.

Field relations show that all the rocks are spatially and temporally related; this evidence alone suggests that they are comagmatic. Some of the chemical trends support comagmatism. However, simple fractional crystallization is not obvious because of large compositional gaps and because some of the more-mafic rocks are nepheline normative.

An AFM plot (fig. 25) and selected silica variation diagrams (figs. 26, 27, and 28) show somewhat continuous trends. Silica concentrations range from 48 to almost 80 percent SiO_2. Values above about 77.5 percent SiO_2 are probably a result of silicification (Hildreth, 1981). Gaps exist between about 48 and 59 percent and 65 and 70 percent. If the late trachytes, represented by sample 81-113, are not related to the caldera, then the second gap is really between 61 and 71 percent SiO_2.

Almost all the chemical variation demonstrated by rocks of the Van Horn Mountains caldera occurs in the intrusive-extrusive suite. That is, all other rocks, including the precollapse rhyolite, rhyolite porphyry, and the two ash-flow tuffs, are rhyolites and mostly high-silica rhyolites. Rocks of this study can be viewed as two groups: rhyolites, which have a very narrow silica range, and the intrusive-extrusive complex, which

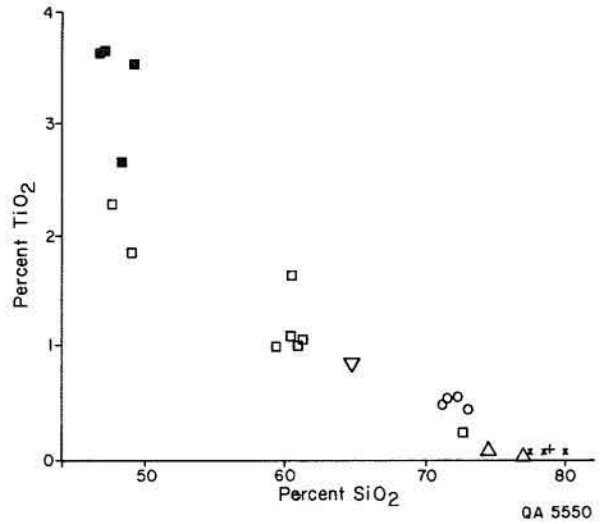

FIGURE 27. Harker variation diagram of TiO_2 plotted against SiO_2. Symbols are explained in figure 25.

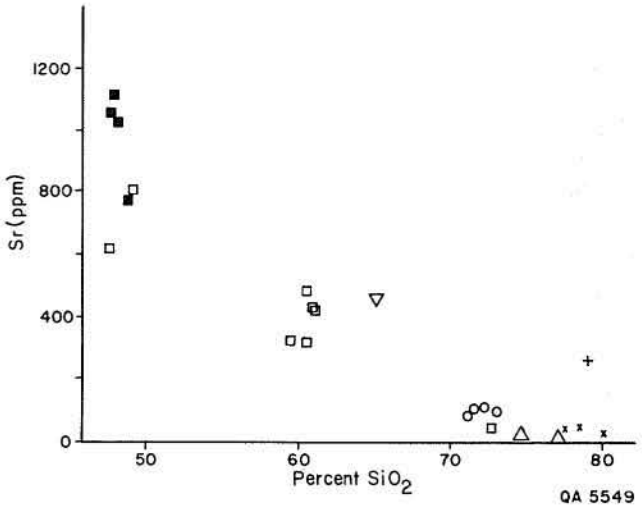

FIGURE 28. Harker variation diagram of Sr plotted against SiO_2. Symbols are explained in figure 25.

varies from 47 to 76 percent SiO_2. The intrusive-extrusive complex, although compositionally more variable, still contains the two compositional gaps mentioned above.

The origin of the compositional gaps is problematic. Many outcrops of the intrusive-extrusive complex are highly weathered or deuterically altered and are not suitable for analyses. More complete sampling might lessen or eliminate the gaps. Alternatively, if the gaps represent the real absence of rocks of the appropriate compositions, a variety of explanations are possible. Baker (1968), Cox and others (1969), and Clague (1978) suggest several magmatic processes that could lead to gaps between basalt and trachtye. Parker (1983) attributed a similar gap in presumably genetically related basalts and trachytes of the Paisano Pass volcano in the nearby Davis Mountains to the failure of conventional indices such as SiO_2 to adequately measure differentiation.

A more serious problem arises from examination of the six analyzed samples of basalt. All are hawaiites by the classification of Barker (1979), which uses the Thornton-Tuttle differentiation index and normative plagioclase compositions. Three of these samples (samples H84-8, H84-10, and H84-12) are nepheline normative (table 1), and a fourth (sample 82-92), although not nepheline normative, shares other characteristics. All four samples have distinctly higher Fe/Mg (fig. 25), higher total alkalis and lower CaO and MgO (fig. 26), higher TiO_2 (fig. 27), and higher Al_2O_3 than the two other basalts, samples 81-192 and 81-200. The four samples also have seemingly higher Sr, but with some overlap (fig. 28), and higher differentiation indices. The other two basalts are both hypersthene-olivine normative, as is sample 82-92. Correction for oxidation or for the presence of CO_2, as is done in the Irvine and Baragar (1971) classification scheme, reduces the amount of hypersthene in the norm. In fact, sample 81-200 becomes very slightly nepheline normative (0.03 percent) using this correction; sample 81-192 remains hypersthene normative. Nevertheless, the other geochemical characteristics remain distinctive.

The significance of the difference in the normative compositions is uncertain. Because all six samples are just about at silica saturation, minor adjustments in CO_2 or Fe_2O_3/FeO can shift the results to show either normative nepheline or hypersthene. Nevertheless, the distinctive chemical characteristics show that there are two different basalts. The differences are probably not a result of differentiation of one to the other; for example, higher alkalis in the four samples would suggest that they are more differentiated, whereas lower TiO_2 in the other two samples suggests that they are more differentiated. Assuming that the differences in silica saturation are real, the four more-alkalic samples should not be able to differentiate to the quartz-normative and quartz-bearing rocks. The two less-alkalic rocks could have. Two distinct magma sources and chambers must have existed at the same time.

Sample 82-89 of a trachyte dike from northeast of the caldera shares several characteristics with the nepheline-normative basalts. It has a higher Fe/Mg (fig. 25), higher TiO_2 (fig. 27), and possibly lower CaO (fig. 26) relative to other trachytes. However, it is distinctly quartz normative.

Field relations are used to argue that all rocks of the intrusive-extrusive complex are related and erupted from the same intrusive source on the eastern side of the caldera. Clearly, dikes could be the source for some of the nepheline-normative rocks. Also, only sample 81-192 was collected near the intrusion. Additional, more detailed field work is warranted to determine precise relationships among these rocks.

A similar conclusion about two distinct magmas has been reached in three other studies of Trans-Pecos Texas. Barker (1977) found both nepheline- and quartz-bearing rocks in the Diablo Plateau intrusive belt. Investigation of the Paisano Pass volcano showed an alkalic basalt-phonolite trend along with a more dominant rhyolitic trend (Parker, 1983). Price and others (1986) show that the Marble Canyon stock is zoned from a nepheline-bearing hawaiite margin to a quartz syenite core, a relationship that suggests mixing of two distinct magmas. All these studies are of the eastern alkalic belt (Barker, 1979), where undersaturated rocks are relatively abundant. To our knowledge, this is the first study to identify two different trends among the mid-Tertiary rocks of the western belt.

Because of compositional gaps and uncertainties about possible parental magmas, any statement about differentiation or relationships between the rocks is premature. Detailed petrologic study to determine the origin of the two trends is underway and will be reported elsewhere.

STRUCTURE

Twiss (1959a) recognized five main events in the structural history of the Van Horn Mountains:

(1) Precambrian (Grenville) metamorphism and folding
(2) Late Pennsylvanian–Early Permian (Ouachita–Ancestral Rocky Mountains) uplift
(3) Late Cretaceous–early Tertiary (Laramide) folding and thrusting
(4) Middle Tertiary volcanism and intrusion
(5) Miocene–Recent (Basin and Range) normal faulting.

Structural trends established during one episode of deformation appear to have been reactivated during later episodes.

Precambrian Deformation

Folding, metamorphism, pegmatite intrusion, and quartz veining in the Carrizo Mountain Group were broadly contemporaneous (King and Flawn, 1953; Davidson, 1980) at approximately 1,000 mya (Denison, 1980). At exposures in the Van Horn, Carrizo, Eagle, and Wylie Mountains, Flawn (1951) and King and Flawn (1953) demonstrated that foliation in metamorphic rocks, contacts between lithologic units, and trends of pegmatite bodies and quartz veins generally strike northeast. At least two periods of deformation are recorded by the two major trends in strike: approximately N. 50° to 70° E. and N. 25° to 45° E. At the well-exposed outcrops in the Mica Mine area northwest of the caldera, the latter trend dominates (Flawn, 1951), and although exposures are poor in the northeastern Van Horn Mountains, both trends are also recognized (King and Flawn, 1953).

The northeast-striking foliations in the Carrizo Mountain Group generally dip to the southeast and may be related to thrusting and recumbent folding. An overturned anticline is the major structural feature mapped by Flawn (1951) in the Mica Mine area. At the northern end of the Carrizo Mountains approximately 29 km north of the Van Horn Mountains caldera, rocks of the Carrizo Mountain Group are thrust over less metamorphosed sedimentary and volcanic rocks of the Allamoore Formation (King and Flawn, 1953). Roughly southward-plunging lineations in metarhyolite of the Carrizo Mountain Group and roughly eastward-striking fold axes in the younger Precambrian rocks in the vicinity of the overthrust suggest northward thrusting. Whether or not the Carrizo Mountain Group in the Van Horn Mountains is allochthonous is uncertain.

Late Pennsylvanian - Early Permian Uplift

Uplift related to Ouachita - Ancestral Rockies deformation exposed rocks of the Carrizo Mountain Group to erosion during the Late Pennsylvanian to Early Permian. Conglomerates and sandstones in the Powwow Member of the Hueco Limestone were derived from these exposures and deposited at the same time. On the basis of thicker Permian marine sequences to the east, Twiss (1959a) considered the Van Horn Mountains to have been located in the core of the Van Horn Uplift, a structural high that persisted at least into Cretaceous time. The Van Horn Mountains caldera lies near the southern margin of this uplift. The caldera is situated adjacent to the southernmost exposures of Precambrian rocks in Trans-Pecos Texas, and for a distance of approximately 90 km south of the caldera, Cretaceous

and younger units cover any Permian rocks in the subsurface.

Laramide Folding and Thrusting

Laramide deformation, which occurred dominantly in Late Cretaceous and early Tertiary time, is responsible for some of the tilting, folding, and faulting of Cretaceous and earlier rocks in the Van Horn Mountains. The deformation predates most of the igneous activity in Trans-Pecos Texas, which occurred chiefly between 38 and 32 mya (Henry and McDowell, 1986). Tertiary volcanic rocks generally dip less steeply than the tilted Cretaceous sedimentary rocks. Contemporaneity of the waning stages of Laramide deformation with middle Tertiary volcanism is suggested by regional dike and vein orientations (Price and Henry, 1984).

Laramide thrust faulting and folding is more obvious in the southern Van Horn Mountains than near the caldera. Twiss (1959b) noted that thrusting, with directions of transport dominantly from west to east, appears to end near the western margin of the Van Horn Mountains. The caldera thus lies near the boundary between the mobile Chihuahua Tectonic Belt to the southwest and the stable Diablo Platform to the northeast (fig. 1).

A north-northwestern to northern structural trend, which is defined by fold axes and thrust faults (Twiss, 1959a), was established during Laramide deformation. In addition, the northeastern structural grain of the Precambrian deformation may have been reactivated at this time. Similarly trending faults in the Indio Mountains (Underwood, 1963) and southern Quitman Mountains (Jones and Reaser, 1970) to the west have distinct strike-slip displacements, but in the Van Horn Mountains, most faults with this trend exhibit normal displacements and probably formed during Miocene to Recent Basin and Range deformation (Twiss, 1959a). Faults of both the north-northwestern to northern and the northeastern trends locally appear to control the northern and western boundaries of the Van Horn Mountains caldera (see plate) and may be reactivated Laramide structures.

Caldera Structure

The topographic wall of the Van Horn Mountains caldera is well exposed through more than 270° of arc (fig. 2; plate); only the southeastern rim is buried beneath postcaldera rocks. The caldera boundary is roughly circular, is only 4 km in diameter, and has numerous embayments. In places the caldera boundary followed or was influenced by older, probably Laramide, faults. The central, subsided block is not exposed, although some highly brecciated masses of Cretaceous rock along the northwestern boundary could represent part of the block. Thus the exposed topographic rim is an eroded scarp of the caldera fault and not the actual fault.

The following description of the caldera boundary begins along the northern edge, directly north of High Lonesome Peak, and continues clockwise around the caldera. At this location the boundary is least complex, consisting of topographically low Hogeye Tuff within the caldera basin lapping against higher Cox Sandstone in the wall. The contact is poorly exposed because Hogeye Tuff is generally nonresistant. The boundary continues beneath the ridge east of High Lonesome Peak, where it is buried beneath lava flows and the High Lonesome Tuff.

South of this ridge to just south of Carpenter Lodge, the caldera boundary may consist of two approximately concentric faults (see plate). The western edge of precaldera Buckshot Ignimbrite outcrop marks the approximate line of the major inner fault. Within this boundary, precaldera rocks are not exposed; at the southern end of it, tuff-breccia is deposited against the Buckshot Ignimbrite.

The outer, lesser fault is more speculative, but may be marked by the contact between Cretaceous rocks on the east and the Buckshot Ignimbrite on the west (see plate). The Cretaceous rocks on the upthrown side of this speculative boundary dip into the caldera as much as 35°. The Buckshot crops out at much lower elevations just west of the Cretaceous rocks. Either it was dropped down along a fault or filled a steep paleovalley formed before caldera collapse. The small outcrop of Cox Sandstone at this boundary consists of jumbled boulders of sandstone and limestone up to 2 m in diameter. Although no tuff matrix was observed, these boulders may be similar to the tuff-breccia exposed in the western part of the caldera. The northwest-trending outcrop of Buckshot Ignimbrite at Carpenter Lodge dips to the north, generally toward this outer collapse zone, whereas Buckshot capping the hill to the south is flat lying. The dipping Buckshot either was deposited that way against the wall of a paleovalley or was tilted by caldera collapse.

Tuff-breccia juxtaposed against Cretaceous rocks marks the southern caldera boundary from Carpenter Lodge around to the western edge where the stream drains out of the caldera (fig. 29). Cretaceous rocks in the caldera wall are generally topographically higher than the softer breccia within the caldera. The breccia and younger rocks have probably been extensively eroded from within the caldera. Along the southwestern caldera wall, tuff-breccia crops out at an elevation 150 m above the topographically lowest exposure of tuff-breccia in the caldera basin. Just southwest of Carpenter Lodge a large block of Buckshot Ignimbrite

FIGURE 29. Western topographic wall of caldera. Light-colored rock in low ground is tuff-breccia. The dike on the left is a basalt of the intrusive-extrusive complex.

and precaldera rhyolite is surrounded by breccia; the block slumped into the caldera from the adjacent wall.

The northwestern boundary of the caldera is complex. Tuff-breccia lies against Cretaceous rocks similar to the situation along the southern margin. However, much of the Cretaceous rock, which is dominantly Cox Sandstone, is intensely brecciated and, by our interpretation, is within the caldera. The character of these brecciated rocks varies considerably in degree of brecciation and in presence and amount of tuffaceous matrix. One hill of Cox Sandstone, striking northeast and dipping 25° northwest (see plate), seems simply to have slumped into the caldera as a displaced but coherent block. In places, generally farthest from the center of the caldera, the rocks are internally fractured but not extensively displaced relative to each other; the original sedimentary layering can be traced roughly through them. With an increase in intensity of brecciation, rocks are displaced relative to each other, layering becomes indistinct, and the character of the rock, beyond simple lithology, becomes unclear. In the most intensely brecciated rocks, diverse lithologies are juxtaposed in random orientations (fig. 15).

The rocks grade continuously from fractured sandstone to tuff-breccia with sandstone and other clasts. As the intensity of brecciation increases, a matrix of tuff-breccia appears and becomes a prominent constituent. The least deformed rocks have no matrix. The most deformed have as much matrix as clasts, and the tuff-breccia is itself a further development of this trend, having a few large, scattered clasts in an almost entirely volcanic matrix. The point at which matrix first appears is not easy to identify because the tuff-breccia is nonresistant. Outcrops are dominated by the more resistant Cretaceous rocks, particularly fragments of Cox Sandstone. Only Cretaceous rocks can be seen on aerial photographs or from a distance, and a general stratigraphic order is preserved in at least one location. Except for the lack of continuous bedding, the outcrops would be interpreted as undisturbed Cretaceous.

The origin of these brecciated rocks is clearly tied to caldera formation. Laramide deformation has also brecciated the Cretaceous rocks, and some of the brecciation observed may be related to Laramide folding or faulting. However, we have observed the intense brecciation described above only adjacent to the caldera. We believe that these rocks slumped into the caldera, at least during formation of the tuff-breccia, but possibly also during initial caldera subsidence. The most intensely deformed rocks, and clearly those with any volcanic matrix, must have formed after initial subsidence. They were deposited by landslides from the oversteepened caldera wall. The landslide blocks disaggregated and became randomly oriented in a volcanic matrix. Brecciated rocks with no volcanic matrix are probably also large landslide blocks that simply did not disaggregate sufficiently to allow incorporation of a volcanic matrix. Less likely, they may

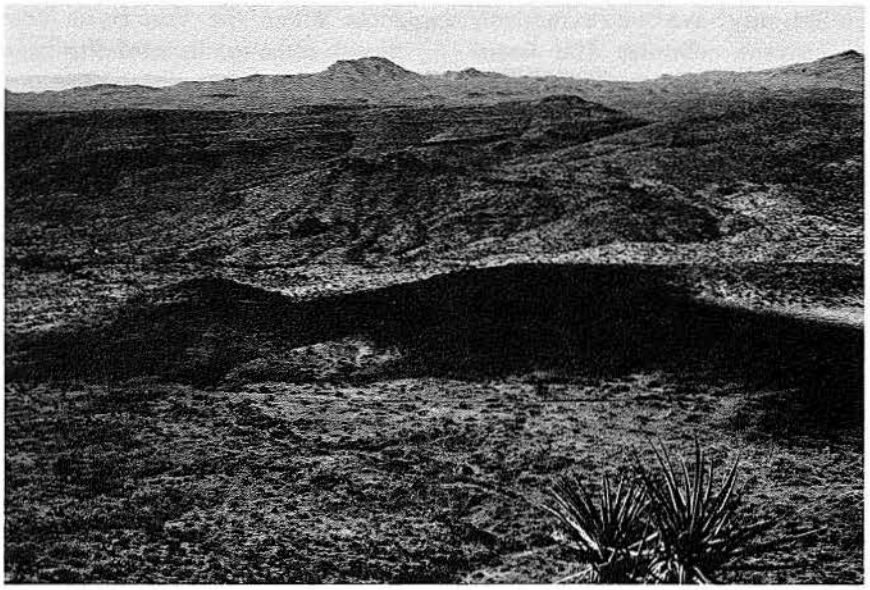

FIGURE 30. Large slump block of Cretaceous rocks along western caldera wall. Slump is ragged ridge in middle ground and consists of Cox Sandstone dipping 25° to northwest into less steeply dipping sandstone in caldera wall.

have slumped into the caldera during initial formation and before the tuff-breccia was deposited. If so, they could have incorporated ash-flow tuff.

We have chosen the contact between undeformed precaldera rocks and similar but brecciated rocks to mark the caldera boundary because it is the limit of caldera-related deformation. From the description above, it is clear that in places this contact simply marks where blocks fell into the caldera (fig. 30). In part, the contact follows precaldera faults or other structures; in part, the contact appears to be gradational and may be more of a hingeline. For example, the large (1.5 × 0.5 km), wedge-shaped breccia block in the northwestern corner of the caldera is bounded on the southwest by a normal fault and on the northwest by a gradational contact with undeformed Cox Sandstone. A traverse along the northeast-trending arroyo through the middle of the block from the fault to the tuff-breccia illustrates the complexity of the caldera boundary. The fault divides unbrecciated Hueco Limestone outside the caldera from highly fractured Cox Sandstone within the caldera on the northeast side of the fault. At the fault the Cox is fractured but is still in place. Halfway to the tuff-breccia, fracturing is much more intense and only the crudest layering can be observed. Near the contact with tuff-breccia, the block consists of randomly oriented fragments of Cox Sandstone or, right at the contact, Finlay Limestone, in a volcanic matrix. This block may have slumped into the caldera along a hingeline at the gradational contact and been displaced along the northwest-trending fault. The fault continues to the northwest well beyond the caldera so it must have a noncaldera origin. Basin and Range faulting may have further reactivated the fault.

Although we have chosen the above contact as the caldera boundary, the contact probably does not have significant displacement where it is a hingeline. Major displacement during initial caldera subsidence probably occurred along what is now the contact between brecciated precaldera rocks and the tuff-breccia.

Except for the "landslide" blocks and the speculative concentric faults along the eastern margin, the caldera boundary seems to have been a single, nearly circular collapse zone. Initial subsidence must have been almost entirely along this single zone with later modifications caused by slumping along the oversteepened caldera wall. The caldera boundary, particularly the subsequent slump features, was strongly influenced by precaldera structures. The caldera boundary, as we define it, is highly embayed along north and northwest trends.

The rhyolite porphyry is a central intrusion similar to resurgent domes of many calderas described by Smith and Bailey (1968). However, the rhyolite porphyry does not clearly uplift the intruded rocks. The general lack of layering in the tuff-breccia may disguise uplift, but it appears that the rhyolite simply intruded through the breccia. This lack of uplift may indicate that the caldera

floor, which is totally buried, may have been extensively broken during initial caldera collapse. The linear contacts of much of the rhyolite porphyry and tuff-breccia, which lie along continuations of trends of precaldera faults, suggest that brecciation of the caldera floor channeled emplacement of the rhyolite porphyry. Dismemberment of the floor allowed the rhyolite to intrude through it without having to uplift it. Brecciation of the caldera floor is indicated both by highly brecciated blocks along the wall and, possibly more importantly, by the abundant precaldera faults trending toward the caldera. Laramide or older faults may have sufficiently divided the caldera area before collapse so that the floor broke along the faults during collapse. If this hypothesis is correct, the Van Horn Mountains caldera may be unlike most calderas in which the central block subsided largely unbroken (Lipman, 1984).

The underlying magma chamber apparently did not dome precaldera rocks. Attitudes of the older rocks show no consistent relationship to the caldera. Probably the attitudes are all a result of Laramide and other precaldera events.

Basin and Range Deformation

Basin and Range normal faulting, which postdates the voluminous Tertiary volcanic activity in Trans-Pecos Texas, probably began about 23 mya (Muehlberger, 1980; Henry and Price, 1986) and continues into the Recent (Baker, 1934a; Muehlberger and others, 1978; Dickerson, 1980). Approximately 26 km south of the Van Horn Mountains caldera, basaltic dikes that intruded along structures associated with the Rim Rock Fault, the large normal fault forming the western boundary of the Van Horn Mountains, are 19 to 24 m.y. old (Dasch and others, 1969; Henry and Price, 1986). Quaternary scarps occur along the major fault that separates the Van Horn Mountains from Lobo Valley to the east (Muehlberger and others, 1978).

Basin and Range deformation was chiefly extensional, although some strike-slip motion has been documented (Dumas and others, 1980). Twiss (1959a) mapped three major trends in strike of Basin and Range normal faults in the Van Horn Mountains: (1) a north-northwestern to northern trend, parallel and subparallel to the Rim Rock Fault, (2) a north-northeastern trend, roughly parallel to the eastern boundary of the northern Van Horn Mountains, and (3) a northeastern trend. Easterly and northwesterly striking faults are also locally abundant (Twiss, 1959a). Substantial vertical displacements, as much as 900 m, are indicated for faults of the north-northwestern to northern trend, which may be a reactivation of the major Laramide trend. One normal fault west of High Lonesome Peak clearly displaces Oligocene volcanic rocks within the Van Horn Mountains caldera (see plate), although its total displacement is no more than about 70 m. Most others appear either to be truncated by the caldera boundary or to die out towards the caldera. Some of these faults are probably of Laramide origin. However, some are Basin and Range faults, either new faults or reactivated Laramide faults; the fact that they do not cut the caldera indicates that the underlying solidified magma chamber served as a buttress to prevent faulting. Faults of the north-northeastern and northeastern trends are subparallel to the two main trends of Precambrian structures in the area. The northeastern trend may also have been reactivated during Laramide and Ouachita deformation (Twiss, 1959a). Faults of the north-northeastern and northeastern trends commonly terminate against and locally displace faults of the north-northwestern to northern trend (Twiss, 1959a; Price, 1982).

ECONOMIC GEOLOGY

Several deposits of economic interest occur in the Van Horn Mountains, but only meager evidence of metallic mineralization directly related to Tertiary igneous activity has been recognized. A combination of features, including the small size of the Van Horn Mountains caldera and the chemical compositions of the extrusive and intrusive rocks, may be responsible for the apparent lack or sparsity of igneous-related mineral deposits.

Hydrothermal Alteration Associated with the Rhyolite Porphyry of the Van Horn Mountains Caldera

Evidence of hydrothermal alteration and minor mineralization occurs in the western part of the caldera, where the rhyolite porphyry is commonly hydrothermally altered, and samples of rhyolite porphyry with stockwork quartz veinlets have been found in float. The rhyolite porphyry is extensively silicified, and feldspar phenocrysts are partly altered to sericite and a kaolinite group mineral. Chemical analyses (table 1) of the rhyolite confirm both the silicification and redistribution of alkalis.

Although the samples of stockwork veinlets are oxidized, traces of pyrite can be observed in polished sections. Chemical analyses (table 2) indicate enrichments in molybdenum and silver. The high potassium content in sample D suggests potassic alteration, consistent with sericitization seen in other parts of the

TABLE 2. Chemical analyses of rhyolite porphyry with stockwork quartz veinlets, Van Horn Mountains (ppm).*

Element	Sample A	Sample B	Sample C	Sample D	For Comparison—Average Granite†
Li	20	1	1	2	40
Be	3	3	<1	2	3
F	32	49	52	25	810
Na	23,100	22,000	3,900	14,400	24,600
Mg	200	400	60	200	2,400
Al	57,100	57,200	18,500	59,000	74,300
P	<25	<25	<25	<25	600
K	41,200	26,300	22,200	62,100	42,000
Ca	600	6,100	650	180	9,900
Ti	500	400	200	400	1,500
V	<2.5	<2.5	<2.5	<2.5	44
Cr	2	1	2	2	4
Mn	100	200	20	200	390
Fe	3,900	2,300	2,000	6,900	14,200
Ni	3	4	4	5	4.5
Cu	2	1	2	4	12
Zn	40	20	15	40	51
As	<5	<5	<5	<5	2.1
Se	<12.5	<12.5	<12.5	<12.5	0.14
Mo	12.8	8.8	20.2	12.3	1.3
Ag	1.2	2.6	1.2	0.6	0.037
Cd	<1	<1	<1	<1	0.1
Au	<0.04	<0.04	<0.04	<0.04	0.0023
Pb	<10	<10	<10	<10	18
Th	15	15	8	15	20
U	<5	10	<5	<5	3.9

†Values for average granite from Rose and others (1979) and Mason (1966).

*Analyses by inductively coupled argon plasma spectrometer with the exceptions of F (analyzed by specific ion electrode), Mo (analyzed by spectrophotometry with a Zn-dithiol complex extracted into amyl acetate), and Ag and Au (analyzed by graphite furnace atomic absorption spectrometry).

intrusion. Fluid inclusions in quartz veinlets contain as many as six phases: liquid, vapor, halite, sylvite, hematite, and an unidentified opaque mineral. Such high-salinity fluid inclusions are typical of potassic alteration zones in porphyry-molybdenum systems. Outcrops of stockwork quartz veinlets or other mineralized rock have not been discovered. Erosion may have removed a more extensive shell of hydrothermal alteration and mineralization above the rhyolite porphyry. However, field evidence indicates that the rhyolite was emplaced at very shallow depths with little or no overburden; thus any overlying alteration shell must have been thin.

Mica

Muscovite is abundant in pegmatites and mica schists of the Precambrian Carrizo Mountain Group in the Mica Mine area northwest of the caldera. Flawn (1951) reported that attempts were made to extract mica from schist between 1920 and 1930 and that approximately $5,000 worth of mica from pegmatites was sold during World War II. In 1981, the Alamo Mica Company began production of mica from schist using a dry-separation mill. The product is used in controlling circulation of drilling fluids in the oil and gas industry.

Building Stone and Crushed Rock

At a locality within the Van Horn Mountains caldera, 0.9 km southwest of High Lonesome Peak, banded tuffaceous sedimentary rock from the Hogeye Tuff has been quarried for building stone. Limestone for railroad ballast and road metal has been quarried in the

Van Horn Mountains from the Hueco Limestone 10 km northeast of the caldera and from the Buda Limestone 16 km to the southeast. Quaternary terrace gravel has also been extracted near the latter locality.

Manganese and Barite

The Mayfield prospect, a psilomelane-barite occurrence, is located 16 km southeast of the caldera. Only one carload of hand-picked manganese ore is reported to have been shipped from the prospect (Baker, 1934b). Ore minerals occur along the northwestward-striking Mayfield Fault, the Basin and Range normal fault that forms the southeastern boundary of the Van Horn Mountains. King and Flawn (1953) noted the presence of barite along the Rim Rock Fault in the Mica Mine area, and Price (1982) described similar occurrences 3 km to the north along the same fault and along other Basin and Range faults.

Price (1982) suggested that all of these barite deposits formed from the oxidation of sulfide-rich (and locally manganese-rich) waters moving upward along faults to shallow depths. The source of the barium could have been either from deep or shallow waters. No connections with igneous activity are apparent at these localities; there are neither intrusive nor extrusive rocks associated with the mineralization.

Silver and Other Metals

At the Plata Verde Mine approximately 6 km northeast of the Van Horn Mountains caldera, small silver deposits occur in sandstones of the Powwow Member of the Hueco Limestone (Twiss, 1959a). Price (1982) reported that production from 1934 to 1943 totaled 16,000 short tons of ore averaging 0.059 percent silver, 0.38 percent copper, and 0.14 percent lead. Relative to unmineralized Powwow sandstones, the ore is also enriched in arsenic, molybdenum, zinc, and cadmium. Nearly all of the ore is confined to reduced rocks or rocks that were once reduced and are now limonitic as a result of supergene oxidation. Although some reduction is sedimentary or diagenetic in origin, much of the reduction associated with mineralization occurs near faults and was probably formed by introduction of sulfide-rich waters along Basin and Range normal faults.

Price (1982) proposed a mode of ore deposition similar to epigenetic red-bed copper deposits, whereby metals were transported in low-temperature, oxidizing ground waters through the Powwow red beds. Precipitation of the metals was accomplished by reaction of the oxidizing ground water with sulfide-bearing waters or rocks. Because sulfide introduction into the Powwow sandstones occurred dominantly during Basin and Range faulting, the mineralization postdates Oligocene igneous activity associated with the Van Horn Mountains caldera.

Minor amounts of lead and zinc are apparently associated with the Mayfield barite-manganese prospect (Warren, 1946) and with travertine in a cave 0.4 km southwest of the Mayfield prospect (Baker, 1934b). Neither these occurrences nor the Plata Verde deposits exhibit features that directly link them to the intrusive or extrusive activity in the Van Horn Mountains caldera.

Lack of Major Mineral Deposits Associated with the Van Horn Mountains Caldera

No metallic mineral deposits are known within or related to the Van Horn Mountains caldera. Hydrothermal alteration and possibly minor deposition of molybdenum associated with the rhyolite porphyry are the only evidence for mineral deposition. Small sizes of the caldera and associated intrusions may have been insufficient for the formation of large-scale hydrothermal systems typical of many ore deposits. Some of the larger calderas in Trans-Pecos Texas are associated with igneous-hydrothermal mineral deposits (McAnulty, 1976; Henry and Price, 1984). As examples, lead-zinc-silver veins (Evans, 1975) and tungsten-molybdenum skarns (Murry, 1980) occur in and near the intrusions in the Quitman Mountains 67 km northwest of the Van Horn Mountains caldera; fluorite veins and replacement bodies occur in the Eagle Mountains (Gillerman, 1953) 21 km to the northwest; lead-zinc-silver-fluorite veins, manto silver deposits, and a porphyry copper-molybdenum deposit are associated with the Chinati Mountains caldera 110 km to the south (Duex and Henry, 1981; Cepeda and Henry, 1983). In the Van Horn Mountains caldera, the relatively brief period of igneous activity or the small size of the caldera may have been inadequate for the development of widespread hydrothermal activity and ore deposition.

The chemical compositions of the igneous rocks may also be a cause of the paucity of mineral deposits in or near the caldera. Mineral deposits would not necessarily be expected to be genetically related to the less differentiated trachytic rocks. In addition, the pristine igneous rocks may not have been sufficiently enriched in metals to allow hydrothermal activity to concentrate them.

The lack of recognized deposits could be a function of the level of erosion. All of the intrusive rocks appear to have been emplaced at shallow depths. Gradational

contacts with breccias derived from the rhyolite porphyries in the southwestern part of the caldera suggest that the intrusions were domes whose tops were exposed during emplacement. The aphanitic, flow-banded rhyolite of the intrusion at Garden of the Gods probably solidified rapidly upon intrusion to a shallow level. If any mineral deposits do exist at depth, however, they do not have extensive, obvious surface expressions.

GEOLOGIC HISTORY OF TERTIARY VOLCANISM

The Van Horn Mountains caldera was one of the earlier volcanic centers of Trans-Pecos Texas and probably the earliest in the northwest part of the volcanic field. Nevertheless, volcanism had started earlier, both in the Davis Mountains and in the Infiernito caldera of the Chinati Mountains. The Buckshot Ignimbrite was erupted from the Infiernito caldera (Duex and Henry, 1981); Vieja Group tuffaceous sediments in the Colmena Formation and in the Chambers Tuff below the lower marker horizon had a southern source (Walton, 1972). The Buckshot reached the area of the Van Horn Mountains, where it filled valleys cut into Cretaceous rocks. A surface of significant relief had developed on the Cretaceous rocks resulting from erosion following Laramide folding and uplift.

The time of emplacement of the Garden of the Gods rhyolite is not certain. It is younger than the Buckshot Ignimbrite, which it intrudes, and is clearly older than some caldera-related rocks. We believe that it was emplaced shortly before caldera collapse. Its contemporaneity and proximity to the caldera indicates that it is part of caldera magmatism and probably derived from the same magma chamber that gave rise to the other rocks.

Volcanic activity in the Van Horn Mountains caldera began with eruption of the ash-flow tuff and simultaneous collapse of the caldera. No older locally derived volcanic rocks are known, although they could occur within the caldera beneath the ash-flow tuff. The ash-flow tuff is probably correlative with the lower marker horizon of the Chambers Tuff, which also coincides with a change to a northern source of tuffaceous sediments in the Vieja Group (Walton, 1972). Thus the volcanic and sedimentary records are consistent on the timing and location of volcanism early in the development of the Trans-Pecos field.

The ash-flow tuff definitely accumulated within its own caldera; collapse and eruption were undoubtedly simultaneous. The tuff spread primarily to the south. The site of the caldera and volume estimates of the lower marker horizon indicate that little, if any, tuff could have spread to the north.

Caldera collapse occurred along a roughly circular zone about 4 km in diameter and was coincident with tuff eruption. The collapse zone was in part controlled by older, mostly Laramide structures, and much of the Cretaceous sedimentary rock in the caldera wall is intensely brecciated, probably related to collapse but possibly also inherited from Laramide deformation.

An abundance of igneous activity followed collapse, including continued pyroclastic eruptions, probably as air-fall tuffs, and intrusion of rhyolite porphyry. Pyroclastic activity and intrusion overlapped in time; the tuff-breccia that accumulated within the caldera contains clasts of the rhyolite porphyry and is in turn intruded by the rhyolite. Slumping of the oversteepened wall provided large (up to 50 m) blocks of Cretaceous rocks to the tuff-breccia.

Pyroclastic activity from the caldera subsided, and accumulation within the caldera changed from a tuffaceous breccia to more normal tuffaceous sedimentation. The change was gradual and represented a decline in the proportion of a local tuff component as compared to more regional sources. Early tuffaceous sediments of the Hogeye Tuff were lacustrine and accumulated in a closed basin within the caldera. The closed basin may have covered nearly all of the caldera floor but likely was segmented into several smaller basins by irregular topography on the tuff-breccia and rhyolite porphyry. Eventually fluvial sedimentation became dominant and continued at least until eruption of the High Lonesome Tuff.

The intrusive-extrusive complex was emplaced toward the end of, but concurrently with, tuffaceous sedimentation. The complex was fed largely by a stock outside the eastern margin of the caldera. Flows extended from the source to the north and south and extensively to the west into the caldera. The caldera must still have been a topographic basin at the time. Basaltic, trachytic, and rhyolitic dikes within and outside the caldera were probably emplaced at this time. The sequence of initial rhyolitic pyroclastic and volcanic or intrusive activity followed by trachytic and more-mafic lava flows probably represents tapping of a differentiated magma chamber and is common in calderas of Trans-Pecos Texas. For example, the Chinati Mountains caldera went through three such cycles (Cepeda and Henry, 1983).

Eruption of the High Lonesome Tuff was the second major caldera event. Eruption may have been accompanied by additional subsidence, but evidence is equivocal. The High Lonesome Tuff spread extensively to the south and slightly to the west and east. Volume

TABLE 3. K-Ar ages of rocks of the Van Horn Mountains caldera.

Sample	Rock	Mineral	%K	$\%^{40}Ar^*$	$^{40}Ar^*$ ($\times 10^{-6}$ scc/gm)	Age (m.y. $\pm$ 1 σ)
81-202	Rhyolite porphyry	K-feldspar	10.16	86.7	19.15	45.6 $\pm$ 1.3
			10.15	91.4	17.32	
81-116	High Lonesome Tuff	K-feldspar	3.09	92.5	4.62	36.9 $\pm$ 0.8
			3.11	89.4	4.35	
81-117	High Lonesome Tuff	K-feldspar	4.31	92.5	6.34	38.4 $\pm$ 0.8
			4.33	83.3	6.70	

$\lambda\beta = 4.963 \times 10^{-10}\ yr^{-1}$; $\lambda_{\varepsilon}{}^{+}\varepsilon' = 0.581 \times 10^{-10}\ yr^{-1}$; $^{40}K/K = 1.167 \times 10^{-4}$

*radiogenic

considerations suggest that little tuff could have spread to the north.

Clastic sedimentation continued after eruption of the High Lonesome Tuff, but the tuffaceous component diminished dramatically. Probably the sediments were locally derived from rocks exposed in the caldera wall, but tuff-producing eruptions had largely ceased in the Van Horn Mountains caldera.

The last known volcanic event in the area was eruption of the trachyte lava flows that cap High Lonesome Peak. It is unclear whether these are genetically related to the Van Horn Mountains caldera. Similar trachytes occur in the same stratigraphic position well to the south and west of the caldera. They may represent an unrelated regional event, but they could also be flows erupted from the caldera after it was largely filled, so that flows could spread extensively away from the caldera.

K-Ar ages have been determined for the High Lonesome Tuff and rhyolite porphyry (table 3). Other rocks of the caldera have not been dated because they generally are too altered or do not contain datable phenocrysts (for example, the intrusive-extrusive complex) or because they contain abundant older fragments that could mask their true age (for example, caldera-forming ash-flow tuff). Ages of alkali feldspar separates from two samples of High Lonesome Tuff are 37 and 38 m.y. (table 3).

An age of 46 m.y. determined from a sanidine separate from the rhyolite porphyry is impossibly old. The caldera, and therefore the porphyry, is younger than the Buckshot Ignimbrite, which has been dated at about 37 to 38 m.y. (McDowell, 1979; Henry and McDowell, 1986). The aberrant age may be due to incorporation of excess ^{40}Ar in the porphyry, either through direct incorporation of incompletely degassed Precambrian feldspars or through crystallization of sanidine in a magma with a high partial pressure of ^{40}Ar derived from Precambrian rocks. Although either process seems unlikely, the caldera-forming ash-flow tuff contains abundant Precambrian fragments, including the potassium-rich phases microcline, biotite, and muscovite. Similar incorporation in the rhyolite magma would introduce abundant ^{40}Ar.

The age of the High Lonesome Tuff is consistent, within analytical uncertainty, with the ages of the Buckshot Ignimbrite. Because all other rocks of the Van Horn Mountains caldera formed between eruption of the Buckshot and High Lonesome Tuff, all caldera-related events must have occurred at about this time and must have taken no more than 1 m.y.

CALDERA SIZE AND ASH-FLOW TUFF VOLUMES: Implications for Eruption and Subsidence

Comparison of the volumes of erupted ash-flow tuff with the volume (area and amount of subsidence) of the caldera is informative. In this discussion, we first consider the estimated volumes of tuff and their implications for subsidence; second, we infer the paleotopography of the caldera area before eruption to evaluate both volumes and subsidence.

The area of the caldera (10 km^2) is well constrained. In contrast, the estimated volumes of erupted ash-flow tuff are much more approximate (2 to 30 km^3 of outflow caldera-forming tuff, roughly 2 to 3 km^3 of the same tuff within the caldera, about 1 km^3 of intracaldera High Lonesome Tuff, and 2 to 10 km^3 of

outflow High Lonesome Tuff). In calculating subsidence, we assume that collapse is proportionate to the volume of magma erupted as ash-flow tuff; that is, no voids are left within the magma chamber, and remaining magma does not rise sufficiently rapidly to cancel some collapse. We also assume no significant uplift of the subsided block during resurgence, a realistic assumption because the rhyolite porphyry does not seem to have caused any uplift. Regardless, the rhyolite porphyry could not have affected the High Lonesome Tuff, which is younger.

Initial eruption of 2 km^3 of outflow tuff requires about 200 m of subsidence; additional subsidence to allow for the postulated thickness of caldera fill could easily increase this value to 500 m. The maximum estimate of 30 km^3 of outflow tuff leads to a highly unreasonable 3 km of subsidence. The caldera would be almost as deep as it is wide, a situation inconsistent with the geometry of modern calderas. Likewise, 300 m of subsidence associated with 1 km^3 of intracaldera and 2 km^3 of outflow High Lonesome Tuff seems possible, but 1.1 km of subsidence is unrealistic. Some value between the extremes but much closer to the lower values seems most realistic; our high volume estimates are unreasonable.

The second approach considers caldera topography at the time of ash-flow eruption (fig. 31). We assume that Basin and Range faulting has not significantly altered relative elevations within the Van Horn Mountains, although absolute elevations and elevations relative to adjacent basins certainly have changed. This assumption is not perfect; some relative elevation changes have probably occurred, but the paucity of Basin and Range faults within the Van Horn Mountains suggests that most changes are insignificant. The one exception involves the large north-trending fault about 2 km east of the caldera (fig. 31). Displacement across this fault seems significant; elevations should not be compared across it.

Several different types of elevation information exist. The elevation of outcrops of Cretaceous rocks gives a minimum elevation at the time of eruption. Precaldera volcanic rocks, mostly the Buckshot Ignimbrite, were deposited on an erosional surface developed on the Cretaceous. The top of these volcanic rocks thus marks the surface immediately before caldera formation. Similarly, the elevation of the basal contact of caldera-related rocks, whether deposited on Cretaceous or older volcanic rocks, also marks the precaldera topography. Erosion following caldera formation could have modified either of the latter two examples. However, except right along the caldera wall where mass wasting would have been particularly rapid, the amount of erosion should not be large. Finally, present-day structural relief and our knowledge of the tectonic events that affected the area provide indirect evidence of elevations.

Figure 31 summarizes the elevation data. Cretaceous rocks crop out at elevations ranging from more than 1,660 m near the eastern wall of the caldera to less than 1,420 m in the southeast and southwest. The Buckshot Ignimbrite and Colmena Formation filled paleovalleys as low as about 1,420 m in the southeast. One such valley trends northwest or west past Carpenter Lodge and into the caldera collapse area. The Buckshot Ignimbrite crops out at 1,560 m just southwest of this valley, apparently on a ridge overlooking the valley. Farther southeast another paleovalley trends, and must originally have drained, northward (fig. 31; plate). Flows of the intrusive-extrusive complex extend north down a paleovalley cut in Cretaceous rocks in the northeast (fig. 31; plate). The High Lonesome Tuff spilled over the eastern caldera rim and also occupied the north-trending valley.

Paleotopography to the west is not as well constrained. The Cretaceous outcrops provide only minimum elevations. Several factors indicate that the west side, particularly the northwestern corner, was considerably higher than any part of the east side. Tributaries draining toward the east indicate the west side must have been high. Permian and Precambrian outcrops just northwest of the caldera indicate that the area was structurally high; probably it was topographically high also. No volcanic rocks crop out there; either they were never deposited there or have been totally removed by erosion. Either alternative suggests the west side was topographically high. A high area to the west is consistent with the nature and distribution of Laramide deformation. The Van Horn Mountains are at the northeastern edge of the Laramide fold belt. Higher elevations should be expected within the fold belt. Present-day elevations in Chihuahua are commonly as high as 2,200 m but are not directly comparable because they are separated from the Van Horn Mountains by several major structures. Although Cretaceous strata are nearly flat lying across the caldera area, a greater thickness of Cretaceous rocks may have been preserved on the west side than on the east side immediately before caldera formation.

Together these data provide a good picture of the paleotopography along the eastern margin of the caldera but a much more speculative view of the west side. A major valley trended nearly north-south about 1 km east of the caldera. The intrusive-extrusive complex was emplaced directly in the middle of the valley. One or more tributaries extended west or northwest from the major valley into what was probably a high area now occupied by the caldera. The elevation of Cretaceous rocks in the floor of the major valley suggests that it may ultimately have drained to the

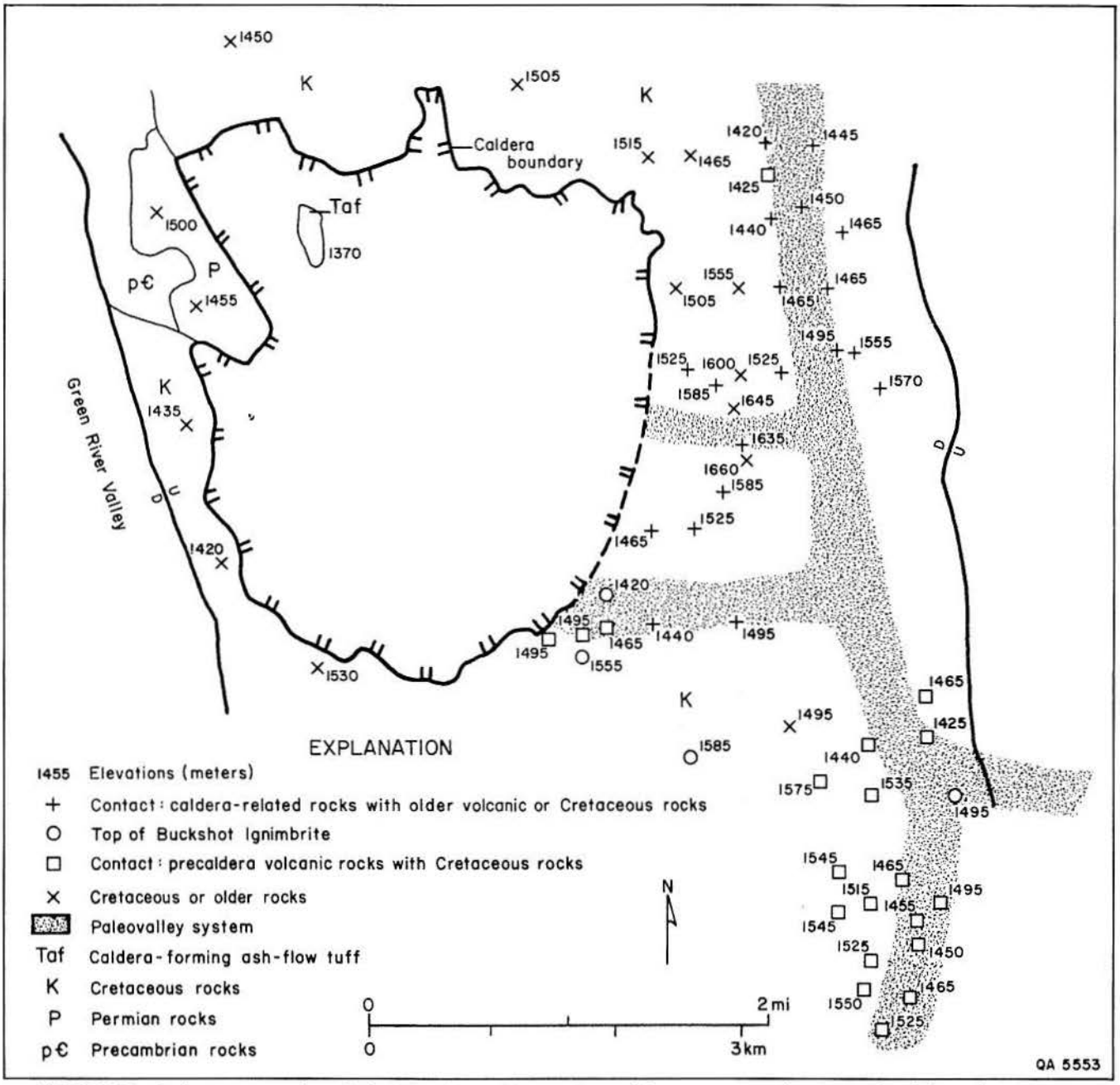

FIGURE 31. Paleotopography of the Van Horn Mountains caldera area at the time of caldera formation.

north. Alternatively, the whole system may have drained east into the present Lobo Valley. The absolute elevation of the west side is speculative but could have been several hundred meters higher than any elevation on the east side. Elevations of as much as 2,000 m are possible. The area had significant relief, as much as a 250-m change in elevation from ridge top to valley in a distance of 1.5 km, comparable to that of present day.

The highest exposed elevation of the caldera-fill ash-flow tuff is about 1,370 m. Because the tuff ponded within the caldera and should not have been eroded while still in a closed basin, 1,370 m is a reasonable elevation for the top throughout the caldera. Tilting related to resurgence or other postcollapse events should be minor. The thickness of underlying tuff may be about 200 to 300 m but cannot be tested by looking at the precaldera topography. The topography can be used to test the volume of outflow tuff and all of the High Lonesome Tuff. Our minimum volume estimate for these rocks, 5 km^3, requires that the caldera wall average about 500 m above the top of the caldera-fill tuff, or about 1,870 m. This value is in fair agreement

with the presumed pre-eruption topography; certainly it does not allow for much larger volumes. Our higher volume estimates are totally unrealistic unless the downdropped block was suspended over a void above the magma or the magma rose rapidly enough to replace the erupted tuff before collapse. Either explanation seems physically impossible.

Almost all ash-flow tuff that escaped the caldera must have flowed to the south. This conclusion is consistent with the presumed topography, the final volume estimates, and the known distribution of both outflow tuffs. Our larger volume estimates allow for a significant component in other directions. Obviously, it is risky to estimate volumes based on very spotty distribution. Apparently the configuration of the caldera wall channeled most of the erupted tuff to the south. A small part of the High Lonesome Tuff is an exception. It passed over the east rim of the caldera and then down the paleovalley both to the north and to the south. It is curious that it flowed over the east rim because the southeast rim at Carpenter Lodge was still apparently the lowest point on the caldera wall.

Ash-flow tuffs are generally acknowledged to form by gravitational collapse of an eruption column (Fisher and Schmincke, 1984). The tuff can flow over topographic barriers whose maximum elevation is a function of the height of the column and the distance of the barrier from the column. No part of the Van Horn Mountains caldera wall should have been high enough to prevent either tuff from overflowing. Nevertheless, the tuffs were channeled to the south, most likely because the southeastern wall was low and led into a major valley system. Apparently topographic relief of at most a few hundred meters can have a significant effect on the direction of flow.

Other topographic features probably also provided constraints. For example, the high Laramide foldbelt formed a western barrier to most tuffs in Texas (Henry and Price, 1984). The Sierra Vieja was a low area in front of the Laramide folds in which both ash-flow tuffs and tuffaceous sediments ponded. However, these constraints were secondary to the topography immediately adjacent to the caldera.

COMPARISON WITH PUBLISHED CALDERA MODELS

The characteristics and development of the Van Horn Mountains caldera generally follow the model of Smith and Bailey (1968) and Lipman (1984). However, it is distinctive in several aspects, most notably size, and comparison with the standard model is informative. Smith and Bailey identified seven major stages of caldera development including (1) regional tumescence, (2) caldera-forming eruptions, (3) caldera collapse, (4) preresurgence volcanism and sedimentation, (5) resurgent doming, (6) ring-fracture volcanism, and (7) hot-spring and hydrothermal activity. They emphasized that stages could be repeated in a cyclic pattern. Lipman (1984) reiterated this model and emphasized precursor volcanism; that is, most calderas are built on earlier volcanoes that are probably part of the same magmatic system.

(1) Regional tumescence and precursor volcanism. Neither of these are observed in the Van Horn Mountains caldera. Precaldera rocks in the wall show a variety of attitudes, from flat lying to gently dipping. However, the rocks clearly do not dip radially away from the center, and the observed dips are easily ascribed to earlier, mostly Laramide, structural events. Possibly the extensive precaldera structural dislocation allowed the underlying magma to rise through the upper crust passively, instead of doming the older rocks.

Precursor volcanism is nonexistent unless extrusive rocks were associated with the Garden of the Gods rhyolite. Because the rhyolite was clearly shallow, it is possible that some magma was extruded, but the resulting flows have been eroded. However, it is clear that the caldera was not built on a substantial earlier volcano. Ash-flow tuff eruption was the first significant volcanism in the area.

(2, 3) Caldera-forming eruptions and collapse. These two stages appear to have been simultaneous, as was ash-flow eruption and caldera collapse in all other calderas in Trans-Pecos Texas (Henry and Price, 1984). It is not known whether collapse breccias occur interbedded with the ash-flow tuff, but their abundance within the overlying tuff-breccia suggests that they do. The collapsed block may have been substantially brecciated during collapse, as indicated by the abundance of precaldera structures that trend into the caldera and by the lack of doming of caldera fill during resurgence. Extensive deformation of what was to become the caldera block during Laramide and earlier events may have allowed it to disaggregate during collapse. In contrast, Lipman (1984) indicates that most calderas subsided as pistons with little internal deformation.

(4) Preresurgence volcanism and sedimentation. As shown by the thick tuff-breccia, post-ash-flow volcanism was extensive. However, the tuff-breccia is contemporaneous with the rhyolite porphyry, which appears to be the counterpart of a resurgent dome in the Van Horn Mountains caldera. Thus the post-ash-flow volcanism is not strictly preresurgence. Nevertheless, the tuff-breccia, along with the lacustrine and fluvial tuffaceous sediments of the Hogeye Tuff and possibly the intrusive-

extrusive complex, seems to occupy the same genetic position.

(5) Resurgent doming. The rhyolite porphyry also occupies an equivalent genetic position to a resurgent dome, even though it does not appear to uplift the intruded caldera-fill. All other calderas of the western alkali-calcic belt in Trans-Pecos Texas have comparable intrusions that also do not commonly uplift the intruded rocks (Henry and Price, 1984). The lack of doming and the apparent influence on emplacement of structures in the subsided block support the idea that it was broken during collapse.

(6) Ring-fracture volcanism. The intrusive-extrusive complex may be an example of ring-fracture volcanism. The intrusive source was emplaced just outside the eastern boundary of the caldera but is not on any observable ring fracture. Certainly no other ring-fracture volcanic rocks are present, and such volcanism is very irregularly developed in other Trans-Pecos calderas (Henry and Price, 1984).

(7) Hot-spring and hydrothermal activity. Hydrothermal alteration of the rhyolite porphyry attests to the former existence of a hydrothermal convection system. Hot springs were probably abundant during volcanism in the caldera. Henry and Price (1984) found that hydrothermal alteration and ore deposition were integral parts of the cycle in most Texas calderas.

The High Lonesome Tuff and possibly the late trachyte lava flows represent a second cycle of stages 2, 3, and 4. Additional caldera collapse during eruption of the High Lonesome Tuff is uncertain, and it is not certain that the trachyte lava flows are derived from the same magma chamber. Nevertheless, the underlying magma chamber clearly went through a second period of replenishment and/or differentiation before eruption of ash flows resumed. Vertical compositional zonation of the caldera-forming ash-flow tuff cannot be investigated with the present incomplete exposures. Zonation is not apparent in the High Lonesome Tuff, which is relatively homogeneous both in major and trace elements (table 1). Although more thorough evaluation is necessary, lack of zonation is notable because small-volume ash flows are more commonly zoned than large ones (Smith, 1979).

Thus the Van Horn Mountains caldera exhibits a reasonably complete sequence of events compared to other resurgent calderas. At the very least, it experienced the critical aspects of ash-flow eruption, caldera collapse, and resurgence, as well as a second cycle of ash-flow eruption. Eruption of two separate ash-flow sheets separated by a significant hiatus indicates two separate, but major, cycles of differentiation of the parental magma. However, the caldera is one of the smallest known to us, with a collapse area of about 10 km^2 and an ash-flow volume of probably no more than 10 km^3. Both these values place it among the smallest of epicontinental ring structures, or ash-flow calderas (Smith, 1979). Indeed, Wood (1984) found no ash-flow calderas under 5 km in diameter; by his criteria, the Van Horn Mountains caldera would be relatively small even for a stratovolcano. The volume is about at the lower limit that would lead to caldera collapse but is roughly proportional to the collapse area, as noted for calderas in general by Smith (1979). Nevertheless, all of its features are those of an ash-flow caldera, not a stratovolcano.

The distribution of Basin and Range faults indicates that the underlying magma chamber is not significantly larger than the collapse structure. As in other Trans-Pecos calderas (Henry and Price, 1984), Basin and Range faults go around the caldera, and faults that trend into the caldera die out rapidly into it. The western boundary fault of the Van Horn Mountains horst lies just 500 m west of the western boundary of the caldera, and another major fault lies just 2 km east of the eastern margin. The magma chamber served as a buttress to resist extension; it must lie entirely between these two faults. We cannot assume that the caldera simply represents a small apophysis of a larger chamber.

Smith (1979) emphasized the variations in diameters of calderas and volumes among ash-flow tuffs and their source magma chambers. Nevertheless, the Van Horn Mountains caldera illustrates several points. Seemingly identical processes occur over a wide range of sizes. Size alone is not a constraint on caldera development, although it may influence exactly how some features, such as resurgence, occur. Significant variations undoubtedly correlate with size, but not in a one-to-one relationship. Lipman (1984) reached a similar conclusion from a much broader sampling of calderas.

Whatever the process that generated the parental magma, it was able to produce very small batches. However, it produced much larger batches elsewhere, if other magmatic systems in Texas formed by similar mechanisms. For example, the Chinati Mountains caldera is approximately 20 km in diameter, and the related caldera-forming ash-flow tuff may be as large as 1,000 km^3 (Cepeda and Henry, 1983). Magma generation for both the Van Horn Mountains and Chinati Mountains calderas probably occurred in the mantle and is related to subduction.

Calderas are commonly difficult to recognize because of their large size. Examination of only a small part of a very large caldera might not reveal any diagnostic features. The smaller size of the Van Horn Mountains caldera made it relatively easy to identify. However, geologists, expecting calderas in general to be much larger, must be careful not to overlook much smaller structures also.

ACKNOWLEDGMENTS

The authors are particularly indebted to P. C. Twiss, who initially studied the geology of the Van Horn Mountains in the late 1950's. His excellent map and thorough descriptions drew us to the area as an appropriate location for a detailed caldera study.

K-Ar ages presented in this report were done in the laboratory of F. W. McDowell, Department of Geological Sciences, The University of Texas at Austin. Chemical analyses were done in the Mineral Studies Laboratory of the Bureau of Economic Geology by S. W. Tweedy. Reviews by D. S. Barker, R. T. Budnik, J. R. DuBar, J. G. Paine, D. F. Parker, and P. C. Twiss greatly enhanced the scientific content of this report.

This report was word processed by Dorothy C. Johnson and Rosanne M. Wilson and typeset by Lisa L. Farnam under the direction of Lucille C. Harrell. Illustrations were prepared by Margaret D. Koenig, Nan Minchow-Newman, and T. B. Samsel III, under the direction of Richard L. Dillon. Text illustration camerawork was by James A. Morgan. The publication was designed by Jamie S. Haynes. Editing was by Michelle C. Gilson.

This research was supported by the Texas Mining and Mineral Resources Research Institute through the U.S. Bureau of Mines, under grant numbers G1124148, G1134148, and G1144148.

REFERENCES

Anderson, W. B., 1975, Cooling history and uranium mineralization of the Buckshot Ignimbrite, Presidio and Jeff Davis Counties, Texas: The University of Texas at Austin, Master's thesis, 135 p.

Baker, C. L., 1934a, Structural geology of Trans-Pecos Texas, *in* The geology of Texas, v. 2: University of Texas Bulletin 3401, p. 137-214.

_____1934b, Manganese minerals and ores, *in* The geology of Texas, v. 2: University of Texas Bulletin 3401, p. 507-508.

Baker, Ian, 1968, Intermediate oceanic volcanic rocks and the "Daly Gap": Earth and Planetary Science Letters, v. 4, p. 103-106.

Barker, D. S., 1977, Northern Trans-Pecos magmatic province: introduction and comparison with the Kenya Rift: Geological Society of America Bulletin, v. 88, p. 1421-1427.

_____1979, Magmatic evolution in the Trans-Pecos province, *in* Walton, A. W., and Henry, C. D., eds., Cenozoic geology of the Trans-Pecos volcanic field of Texas: The University of Texas at Austin, Bureau of Economic Geology Guidebook 19, p. 4-9.

Barnes, V. E., 1979, Geologic Atlas of Texas—Marfa sheet: The University of Texas at Austin, Bureau of Economic Geology, scale 1:250,000.

Cepeda, J. C., and Henry, C. D., 1983, Oligocene volcanism and multiple caldera formation in the Chinati Mountains, Presidio County, Texas: The University of Texas at Austin, Bureau of Economic Geology Report of Investigations No. 135, 32 p.

Clague, D. A., 1978, The oceanic basalt-trachyte association: an explanation of the Daly Gap: Journal of Geology, v. 86, p. 739-743.

Condie, K. C., 1982, Plate-tectonics model for Proterozoic continental accretion in the southwestern United States: Geology, v. 10, p. 37-42.

Coney, P. J., and Reynolds, S. J., 1977, Cordilleran Benioff zones: Nature, v. 270, p. 403-406.

Cox, K. G., Gass, I. G., and Mallick, D. I. J., 1969, The evolution of the volcanoes of Aden and Little Aden, South Arabia: Geological Society of London Quarterly Journal, v. 124, p. 283-308.

Damon, P. E., Shafiqullah, M., and Clark, K. F., 1981, Age trends of igneous activity in relation to metallogenesis in the southern Cordilleran: Arizona Geological Society Digest, v. 16, p. 137-154.

Dasch, E. J., Armstrong, R. L., and Clabaugh, S. E., 1969, Age of Rim Rock dike swarm, Trans-Pecos Texas: Geological Society of America Bulletin, v. 80, p. 1819-1824.

Davidson, D. M., Jr., 1980, Precambrian geology of the Van Horn area, Texas, *in* Dickerson, P. W., and Hoffer, J. M., eds., Trans-Pecos region, southwestern New Mexico and West Texas: New Mexico Geological Society 31st Field Conference Guidebook, p. 151-154.

DeFord, R. K., 1958, Tertiary formations of Rim Rock Country, Presidio County, Texas: Texas Journal of Science, v. 10, p. 1-37.

DeFord, R. K., and Haenggi, W. T., 1970, Stratigraphic nomenclature of Cretaceous—the geological framework of the Chihuahua Tectonic Belt, rocks in northeastern Chihuahua: West Texas Geological Society, p. 175-196.

Denison, R. E., 1980, Pre-Bliss (p€) rocks in the Van Horn region, Trans-Pecos Texas, *in* Dickerson, P. W., and Hoffer, J. M., eds., Trans-Pecos region, southwestern New Mexico and West Texas: New Mexico Geological Society 31st Field Conference Guidebook, p. 155-158.

Denison, R. E., and Hetherington, E. A., Jr., 1969, Basement rocks in far West Texas and south-central New Mexico, *in* Kottlowski, F. E., and LeMone, D. V., eds., Border stratigraphy symposium: New Mexico Bureau of Mines and Mineral Resources Circular 104, p. 1-14.

Dickerson, P. W., 1980, Structural zones transecting the southern Rio Grande rift—preliminary observations, *in* Dickerson, P. W., and Hoffer, J. M., eds., Trans-Pecos region, southwestern New Mexico and West Texas: New Mexico Geological Society 31st Field Conference Guidebook, p. 63-70.

Duex, T. W., and Henry, C. D., 1981, Calderas and mineralization: volcanic geology and mineralization in the Chinati caldera complex, Trans-Pecos Texas: The University of Texas at Austin, Bureau of Economic Geology Geological Circular 81-2, 14 p.

Dumas, D. B., Dorman, H. J., and Latham, G. V., 1980, A reevaluation of the August 16, 1931, Texas earthquake: Bulletin of the Seismological Society of America, v. 70, p. 1171-1180.

Evans, T. J., 1975, Gold and silver in Texas: The University of Texas at Austin, Bureau of Economic Geology Mineral Resource Circular 56, 36 p.

Fink, J. H., 1983, Structure and emplacement of a rhyolitic obsidian flow: Little Glass Mountain, Medicine Lake Highland, northern California: Geological Society of America Bulletin, v. 94, p. 362-380.

Fisher, R. V., and Schmincke, H.-U., 1984, Pyroclastic rocks: New York, Springer-Verlag, 528 p.

Flawn, P. T., 1951, Pegmatites of the Van Horn Mountains, Texas: Economic Geology, v. 46, p. 163-192.

Gillerman, Elliott, 1953, Fluorspar deposits of the Eagle Mountains, Trans-Pecos Texas: U.S. Geological Survey Bulletin 987, 98 p.

Hay-Roe, Hugh, 1957, Geology of Wylie Mountains and vicinity, Culberson and Jeff Davis Counties, Texas: University of Texas, Austin, Bureau of Economic Geology Geologic Quadrangle Map 21, scale 1:63,360, with text.

Heiken, G. B., and Wohletz, K., 1984, Tephra formation during emplacement and destruction of domes (abs.): Geological Society of America, Abstracts with Programs, v. 16, no. 6, p. 536.

Henry, C. D., and McDowell, F. W., 1982, Timing, distribution, and estimates of volumes of silicic volcanism in Trans-Pecos Texas (abs.): Geological Society of America, Abstracts with Programs, v. 14, no. 3, p. 113.

_____ 1986, Geochronology of magmatism in the Tertiary volcanic field, Trans-Pecos Texas, *in* Price, J. G., and others, eds., Igneous geology of Trans-Pecos Texas—Field trip guide and research articles: The University of Texas at Austin, Bureau of Economic Geology Guidebook 23, p. 99-122.

Henry, C. D., and Price, J. G., 1984, Variations in caldera development in the mid-Tertiary volcanic field of Trans-Pecos Texas: Journal of Geophysical Research, v. 89, p. 8765-8786.

_____ 1986, Early Basin and Range development in Trans-Pecos Texas and adjacent Chihuahua: magmatism and orientation, timing, and style of extension: Journal of Geophysical Research, v. 91, p. 6213-6224.

Hildreth, Wesley, 1981, Gradients in silicic magma chambers: implications for lithospheric magmatism: Journal of Geophysical Research, v. 86, p. 10153-10192.

Irvine, T. N., and Baragar, W. R. A., 1971, A guide to the chemical classification of the common volcanic rocks: Canadian Journal of Earth Sciences, v. 8, p. 523-548.

Jones, B. R., and Reaser, D. F., 1970, Geology of southern Quitman Mountains, Hudspeth County, Texas: The University of Texas at Austin, Bureau of Economic Geology Geologic Quadrangle Map 39, scale 1:48,000, 24-p. text.

Keith, S. B., 1978, Paleosubduction geometries inferred from Cretaceous and Tertiary magmatic patterns in southwestern North America: Geology, v. 6, p. 516-521.

King, P. B, 1934, Permian stratigraphy of Trans-Pecos Texas: Geological Society of America Bulletin, v. 45, p. 697-797.

_____ 1965, Geology of the Sierra Diablo region, Texas: U.S. Geological Survey Professional Paper 480, 185 p.

King, P. B., and Flawn, P. T., 1953, Geology and mineral resources of pre-Cambrian rocks of the Van Horn area, Texas: University of Texas Publication 5301, 218 p.

Lipman, P. W., 1984, The roots of ash-flow calderas: windows into granitic batholiths: Journal of Geophysical Research, v. 89, p. 8801-8841.

Mason, Brian, 1966, Principles of geochemistry (3d ed.): New York, John Wiley, 329 p.

Mattison, G. D., and Rudnick, R. L., 1982, Recognition of a Precambrian ash-flow tuff, Van Horn, Texas (abs.): Geological Society of America, Abstracts with Programs, v. 14, no. 7, p. 558-559.

McAnulty, Noel, 1976, Resurgent cauldrons and associated mineralization, Trans-Pecos Texas, *in* Woodward, L. E., and Northrop, S. A., eds., Tectonics and mineral resources of southwestern North America: New Mexico Geological Society Special Publication 6, p. 180-186.

McDowell, F. W., 1979, Potassium-argon dating in the Trans-Pecos volcanic field, *in* Walton, A. W., and Henry, C. D., eds., Cenozoic geology of the Trans-Pecos volcanic field of Texas: The University of Texas at Austin, Bureau of Economic Geology Guidebook 19, p. 10-14.

Muehlberger, W. R., 1980, Texas lineament revisited, *in* Dickerson, P. W., and Hoffer, J. M., eds., Trans-Pecos region, southwestern New Mexico and West Texas: New Mexico Geological Society 31st Field Conference Guidebook, p. 113-122.

Muehlberger, W. R., Belcher, R. C., and Goetz, L. K., 1978, Quaternary faulting in Trans-Pecos Texas: Geology, v. 6, p. 337-340.

Murry, D. H., 1980, Mineralization in the northern Quitman Mountains, Hudspeth County, Texas, *in* Dickerson, P. W., and Hoffer, J. M., eds., Trans-Pecos region, southwestern New Mexico and West Texas: New Mexico Geological Society 31st Field Conference Guidebook, p. 267-270.

Parker, D. F., 1983, Origin of the trachyte-quartz trachyte-peralkalic rhyolite suite of the Oligocene Paisano volcano, Trans-Pecos Texas: Geological Society of America Bulletin, v. 94, p. 614-629.

Peacock, M. A., 1931, Classification of igneous rocks: Journal of Geology, v. 39, p. 54-67.

Picard, M. D., and High, L. R., 1972, Criteria for recognizing lacustrine rocks, *in* Rigby, J. K., and Hamblin, W. K., eds., Recognition of ancient sedimentary environments: Society

of Economic Paleontologists and Mineralogists Special Publication No. 16, p. 108-145.

Price, J. G., 1982, Geology of the Plata Verde Mine, Hudspeth County, Texas: The University of Texas at Austin, Bureau of Economic Geology Mineral Resource Circular No. 70, 34 p.

Price, J. G., and Henry, C. D., 1984, Stress orientations during Oligocene volcanism in Trans-Pecos Texas: Timing the transition from Laramide compression to Basin and Range tension: Geology, v. 12, p. 238-241.

Price, J. G., Henry, C. D., Barker, D. S., and Rubin, J. N., 1986, Petrology of the Marble Canyon stock, Culberson County, Texas, *in* Price, J. G., and others, eds., Igneous geology of Trans-Pecos Texas—Field trip guide and research articles: The University of Texas at Austin, Bureau of Economic Geology Guidebook 23, p. 303-319.

Price, J. G., Henry, C. D., and Standen, A. R., 1983, Annotated bibliography of mineral deposits in Trans-Pecos Texas: The University of Texas at Austin, Bureau of Economic Geology Mineral Resource Circular No. 73, 108 p.

Rose, A. W., Hawkes, H. E., and Webb, J. S., 1979, Geochemistry in mineral exploration (2d ed.): London, Academic Press, 657 p.

Scott, R. W., and Kidson, E. J., 1977, Lower Cretaceous depositional systems, West Texas, *in* Bebout, D. G., and Loucks, R. G., eds., Cretaceous carbonates of Texas and Mexico, applications to subsurface exploration: The University of Texas at Austin, Bureau of Economic Geology Report of Investigations No. 89, p. 169-181.

Smith, R. L., 1979, Ash-flow magmatism: Geological Society of America Special Paper 180, p. 5-27.

Smith, R. L., and Bailey, R. A., 1968, Resurgent cauldrons, *in* Coats, R. R., and others, eds., Studies in volcanology: Geological Society of America Memoir 116, p. 613-662.

Teal, L. N., and Hoffer, J. M., 1980, Petrography and geochemistry of Garren Group volcanic rocks, Chispa Mountain Quadrangle, Culberson and Jeff Davis Counties, Texas, *in* Dickerson, P. W., and Hoffer, J. M., eds., Trans-Pecos region, southwestern New Mexico and West Texas: New Mexico Geological Society Guidebook, 31st Field Conference, p. 241-244.

Twiss, P. C., 1959a, Geology of Van Horn Mountains, Trans-Pecos Texas: University of Texas, Austin, Ph.D. dissertation, 234 p.

_____ 1959b, Geology of Van Horn Mountains, Texas: University of Texas, Austin, Bureau of Economic Geology Geologic Quadrangle Map 23, scale 1:48,000, with text.

Underwood, J. R., Jr., 1963, Geology of the Eagle Mountains and vicinity, Hudspeth County, Texas: University of Texas, Austin, Bureau of Economic Geology Geologic Quadrangle Map 26, scale 1:48,000, 32-p. text.

Walton, A. W., 1972, Sedimentary petrology and zeolitic diagenesis of the Vieja Group (Eocene-Oligocene), Presidio County, Texas: The University of Texas at Austin, Ph.D. dissertation, 264 p.

_____ 1975, Zeolitic diagenesis in Oligocene volcanic sediments, Trans-Pecos Texas: Geological Society of America Bulletin, v. 86, p. 615-624.

_____ 1977, Petrology of volcanic sedimentary rocks, Vieja Group, southern Rim Rock country, Trans-Pecos Texas: Journal of Sedimentary Petrology, v. 47, p. 137-157.

_____ 1979, Sedimentology and diagenesis of the Tascotal Formation: a brief summary, *in* Walton, A. W., and Henry, C. D., eds., Cenozoic geology of the Trans-Pecos volcanic field of Texas: The University of Texas at Austin, Bureau of Economic Geology Guidebook 19, p. 157-171.

Warren, L. E., 1946, Manganese deposits of Texas, *in* Texas Mineral Resources: University of Texas Publication 4301, p. 249-255.

Wood, C. A., 1984, Calderas: a planetary perspective: Journal of Geophysical Research, v. 89, p. 8391-8406.

APPENDIX

Petrographic Descriptions of Chemically Analyzed (CA) or Isotopically Dated (K-Ar) Samples

Precollapse Rhyolite (Garden of the Gods Intrusion)

81-119. Nearly aphyric, flow-banded rhyolitic intrusion. Very minor (<1 percent) 1 mm in diameter phenocrysts of quartz and alkali feldspar in banded groundmass of quartz, alkali feldspar, and minor opaques. Minor vesicles. CA.

81-206. Similar to 81-119, except feldspar phenocrysts are commonly totally dissolved. Segregations of secondary quartz, siderite(?), and minor sericite(?). CA.

Caldera-Forming Ash-Flow Tuff

H84-13. Nonwelded, rhyolitic ash-flow tuff. 10 percent total phenocrysts, dominantly consisting of rounded, embayed quartz as large as 2 mm in diameter and lesser anorthoclase. Also minor plagioclase, oxidized biotite, and opaques. Rare xenoliths of Precambrian rock fragments, microcline, and muscovite and Permian or Cretaceous clastic sedimentary rocks and chert. Some biotite may also be xenocrystic. Groundmass consists of angular and mostly undevitrified glass shards. CA.

Rhyolite Porphyry Intrusion

81-118. 25 percent total phenocrysts, dominantly consisting of 4-5 mm rounded, embayed quartz. Also 1-2 mm plagioclase, 3-4 mm alkali feldspar, and holes that are probably totally dissolved feldspars. Feldspars are commonly silicified and altered to sericite and calcite. Former mafic phenocrysts, probably biotite, totally altered to sericite and opaques. Groundmass consists of a fine mosaic of quartz and cloudy alkali feldspar. CA.

81-207. 20 percent total phenocrysts, dominantly consisting of quartz and sanidine (2.5 mm) with minor plagioclase (1.5 mm). Feldspars are commonly partly dissolved, silicified, and altered to sericite. Minor mafic phenocrysts, probably biotite, altered to opaques and sericite. Trace zircon. Spherulitic groundmass consists of quartz, alkali feldspar, and minor opaques. CA.

81-214. 1.5 mm phenocrysts of embayed quartz (10 percent), alkali feldspar (7 percent), and a plagioclase (3 percent) in a microcrystalline groundmass of quartz and alkali feldspar. Feldspar phenocrysts are commonly silicified and altered to sericite and kaolinite. Minor biotite(?) phenocrysts altered to sericite and opaques. CA.

81-202. 20 percent total phenocrysts of quartz (4 mm), sanidine (3 mm), and oscillatory zoned plagioclase (1 mm). Feldspars relatively unaltered compared to other rhyolite porphyry samples. Former biotite phenocrysts totally altered to opaques and clay minerals(?). Groundmass consists of finely crystalline quartz and alkali feldspar. K-Ar.

Hogeye Tuff

81-186. Detrital rock consisting of grains of quartz, alkali feldspar, plagioclase, pumice, glass shards, and rock fragments. Some shards show axiolitic devitrification; others altered to probable clinoptilolite. CA.

Intrusive-Extrusive Complex

81-120. Rhyolite. Less than 1 percent quartz phenocrysts (0.5 mm) in trachytic groundmass of alkali feldspar, minor plagioclase, opaques, and devitrified glass. Minor calcite in groundmass and abundant irregular vesicles. CA.

82-91. Porphyritic trachyte. 5 percent total phenocrysts, dominantly of clinopyroxene, some of which are zoned, and minor plagioclase and orthopyroxene. Some totally serpentinized grains may have been olivine. Trachytic groundmass consists of plagioclase, clinopyroxene, and opaques with minor calcite. CA.

82-90. Porphyritic trachyte. Similar to 82-91 except slightly fewer phenocrysts and no possible olivine. CA.

81-196. Porphyritic trachyte. 3 percent total phenocrysts of plagioclase, clinopyroxene, orthopyroxene, and magnetite. Some plagioclase slightly altered to calcite; magnetite partly altered to hematite-ilmenite intergrowths. Groundmass of plagioclase microlites, clinopyroxene, and opaques. Minor calcite and chlorite are probably alteration products of glass. CA.

82-89. Porphyritic trachyte dike. 20 percent total phenocrysts of highly fritted plagioclase, lesser clinopyroxene, and minor anorthoclase. Groundmass is a quenched aggregate of plagioclase and clinopyroxene. CA.

81-197. Porphyritic trachyte, similar to 81-196. CA.

82-92. Basalt. 3 percent microphenocrysts (0.3 mm) of plagioclase and olivine. Trachytic groundmass consists of plagioclase laths, clinopyroxene, and opaques with minor calcite. CA.

81-200. Porphyritic basalt. 2 percent total phenocrysts of olivine (1 mm) and clinopyroxene (0.3 mm). Olivine is fractured and partly altered to iddingsite, goethite, and chlorite. Some pyroxenes are zoned and some show a wormy texture. Trachytic groundmass consists of plagioclase, clinopyroxene, olivine, and magnetite. Minor chlorite may be alteration of former glass. Trace pyrite and alteration of magnetite to ilmenite-hematite. CA.

H84-8. Porphyritic basalt dike. Phenocrysts of clinopyroxene, olivine, and plagioclase in groundmass of same minerals and opaques; groundmass and phenocrysts are nearly gradational in size. Plagioclase commonly shows slight normal zoning and has inclusions of clinopyroxene and opaques. Clinopyroxene has partly resorbed core and unaltered edges. Olivine is slightly serpentinized. CA.

81-192. Porphyritic basalt. 10 percent total phenocrysts dominantly of clinopyroxene (up to 3 mm) with 2 percent olivine and plagioclase. Clinopyroxenes are pale gray and zoned and commonly show wormy margins around unaltered cores. Olivine is slightly altered to chlorite, iddingsite, and goethite. Plagioclase is continuous in size with groundmass and contains abundant apatite needles. Groundmass consists of trachytic plagioclase laths, clinopyroxene, olivine, magnetite, and minor ilmenite. Slight calcite in groundmass and some alteration of opaques to ilmenite-hematite. CA.

H84-10. Basalt. Nonporphyritic; groundmass consists of unoriented plagioclase laths, clinopyroxene, olivine, and opaques. Olivine and plagioclase range up to 0.4 mm; clinopyroxene and opaques are about 0.1 mm. CA.

H84-12. Basalt. Similar to 84-10 but with minor altered glass in groundmass and ophitic texture. CA.

High Lonesome Tuff

81-117. Rhyolitic ash-flow tuff, vitrophyre. Phenocrysts of anorthoclase (6 percent; up to 2 mm), plagioclase (5 percent; up to 2 mm), clinopyroxene (including pigeonite and augite; 2 percent; 1 mm), and possible very minor amphibole. Hematite and ilmenite-hematite intergrowths were probably originally magnetite and ilmenite. Trace of zircon and apatite. A single grain of pyrrhotite occurs within clinopyroxene. Groundmass of densely welded shards and pumice is perlitic with minor areas of spherulitic devitrification and a few rock fragments. CA and K-Ar.

81-116. Devitrified, rhyolitic ash-flow tuff. Phenocrysts of anorthoclase (20 percent; to 2 mm) and opaques ($<$1 percent; 0.2 mm). Some possible plagioclase phenocrysts and aggregates of opaques that were probably originally clinopyroxene. Trace of zircon and apatite. Groundmass consists of devitrified, densely welded glass shards and pumice. Some vapor phase crystallization of quartz and alkali feldspar. CA and K-Ar.

81-115. Devitrified, rhyolitic ash-flow tuff. Similar to 81-116 except 10 percent anorthoclase and definite plagioclase. CA.

81-191b. Devitrified, rhyolitic ash-flow tuff. Similar to 81-115. Mafic phenocrysts, probably clinopyroxene, altered to opaques and chlorite. CA.

Late Trachyte of High Lonesome Peak

81-113. Porphyritic trachyte. 2 percent normally zoned plagioclase phenocrysts to 2 mm. Trachytic groundmass of plagioclase, alkali feldspar(?), and opaques. CA.